Inorganic Chemistry

Article

pubs.acs.org/IC

Synthesis and Structures of Cadmium Carboxylate and Thiocarboxylate Compounds with a Sulfur-Rich Coordination Environment: Carboxylate Exchange Kinetics Involving Tris(2-mercapto-1-*t*-butylimidazolyl)hydroborato Cadmium Complexes, $[Tm^{Bu^t}]Cd(O_2CR)$

Ava Kreider-Mueller, Patrick J. Quinlivan, Jonathan S. Owen,* and Gerard Parkin*

Department of Chemistry, Columbia University, New York, New York 10027, United States

Supporting Information

ABSTRACT: A series of cadmium carboxylate compounds in a sulfur-rich environment provided by the tris(2-*tert*-butylmercaptoimidazolyl)hydroborato ligand, namely, $[Tm^{Bu^t}]CdO_2CR$, has been synthesized via the reactions of the cadmium methyl derivative $[Tm^{Bu^t}]CdMe$ with RCO_2H. Such compounds mimic aspects of cadmium-substituted zinc enzymes and also the surface atoms of cadmium chalcogenide crystals, and have therefore been employed to model relevant ligand exchange processes. Significantly, both ^1H and ^{19}F NMR spectroscopy demonstrate that the exchange of carboxylate groups between $[Tm^{Bu^t}]Cd(\kappa^2\text{-}O_2CR)$ and the carboxylic acid RCO_2H is facile on the NMR time scale, even at low temperature. Analysis of the rate of exchange as a function of concentration of RCO_2H indicates that reaction occurs via an associative rather than dissociative pathway. In addition to carboxylate compounds, the thiocarboxylate derivative $[Tm^{Bu^t}]Cd[\kappa^1\text{-}SC(O)Ph]$ has also been synthesized via the reaction of $[Tm^{Bu^t}]CdMe$ with thiobenzoic acid. The molecular structure of $[Tm^{Bu^t}]Cd[\kappa^1\text{-}SC(O)Ph]$ has been determined by X-ray diffraction, and an interesting feature is that, in contrast to the carboxylate derivatives $[Tm^{Bu^t}]Cd(\kappa^2\text{-}O_2CR)$, the thiocarboxylate ligand binds in a κ^1 manner via only the sulfur atom.

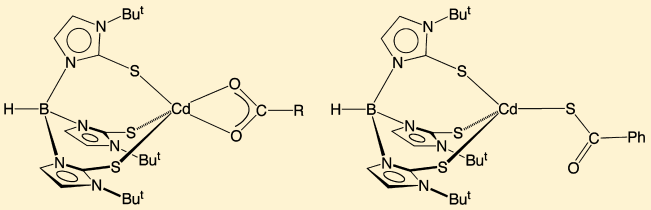

INTRODUCTION

The investigation of cadmium in sulfur-rich coordination environments is of relevance to areas as diverse as cadmium-substituted zinc enzymes[1] and cadmium chalcogenide nanocrystals. With regards to the latter, the surface functionalization of metal chalcogenide nanocrystals via ligand exchange[2] is of considerable importance to their use in applications such as optoelectronic devices and biological imaging.[3] Specifically, the coordination of ligands to nanocrystal surfaces has profound effects on their electronic properties including photoluminescence quantum yield,[4] thermal relaxation of excited carriers,[5] and trapping of electrical carriers.[6] Since carboxylic acids are commonly used as surfactants in the synthesis of cadmium-chalcogenide nanocrystals,[7] the nature of the interaction of the carboxyl group with the nanocrystal surface and the ability to undergo exchange reactions is of considerable importance. In this regard, recent studies concerned with CdSe quantum dots employing oleic acid as the surfactant have shown that (i) the capping ligands are oleate rather than oleic acid, and (ii) the oleate ligands undergo self-exchange with excess oleic acid.[7c] The complexity of nanocrystal surfaces, however, has limited quantitative studies of ligand exchange kinetics.[8,9] Therefore, to provide data of relevance to carboxylate exchange on nanocrystal surfaces, and also the lability of cadmium in sulfur-rich active sites of enzymes, we sought to investigate systems that are more amenable to mechanistic investigations, namely, those of small molecules that feature cadmium in a sulfur-rich environment. In addition, since thiocarboxylates are precursors to cadmium sulfide materials,[10,11] we have also investigated a corresponding thiobenzoate derivative.

RESULTS AND DISCUSSION

Tris(2-mercaptoimidazolyl)hydroborato ligands, $[Tm^R]$ (Figure 1),[12−16] have recently emerged as a popular class of L_2X[17] $[S_3]$ donors that provide a sulfur-rich coordination environment. In this regard, we have previously used the *t*-butyl derivative $[Tm^{Bu^t}]$ to synthesize a variety of zinc,[18,19] cadmium,[20,21] and mercury[22] complexes to investigate aspects of the chemistry of these metals in biological systems, which ranges from the beneficial use of zinc in enzymes to mechanisms of mercury detoxification. An understanding of the kinetics and thermodynamics associated with ligand coordination and exchange involving these metal sites is paramount for fully understanding the chemistry of these systems. Likewise, recognizing that the $[S_3]$ coordination environment of cadmium in $\{[Tm^R]Cd\}$ compounds also resembles the surface metal atoms of the [111] and [001] facets of cadmium chalcogenides

Received: January 4, 2015
Published: March 31, 2015

DOI: 10.1021/acs.inorgchem.5b00017
Inorg. Chem. 2015, 54, 3835−3850

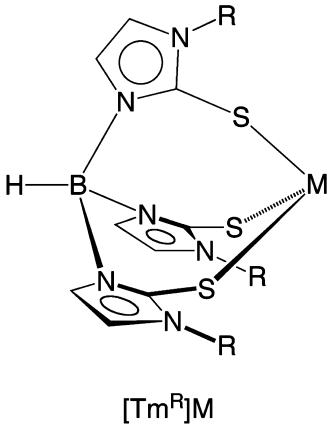

Figure 1. [Tm^{R}] ligands in their κ^3-coordination mode.

with, respectively, zinc blende and wurtzite structures,[23] we rationalized that this class of compounds can also be employed to model ligand exchange processes on cadmium chalcogenide nanocrystal surfaces. Therefore, we have (i) synthesized a series of cadmium carboxylate compounds [Tm$^{Bu^t}$]Cd(O_2CR) and (ii) investigated the dynamics of carboxylate exchange.

1. Synthesis and Structural Characterization of Cadmium Carboxylate Compounds [Tm$^{Bu^t}$]Cd(O_2CR). Although a variety of [Tm$^{Bu^t}$]CdX complexes are known,[20,21,24] there are no reports of structurally characterized carboxylate derivatives.[25] A series of such compounds, namely, [Tm$^{Bu^t}$]Cd(O_2CR) [R = C_6H_4-4-Me, C_6H_4-4-F, C_6H_3-3,5-F_2, C_6H_3-2,6-F_2, 9-anthryl (9-An), n-$C_{13}H_{37}$, and C_3H_6Ph], may, nevertheless, be synthesized via the reactions of [Tm$^{Bu^t}$]CdMe[20] with RCO_2H (Scheme 1). Furthermore, [Tm$^{Bu^t}$]Cd(O_2CR) may also be obtained via reactions of [Tm$^{Bu^t}$]Na[15,26] with cadmium carboxylate compounds as generated by treatment of RCO_2H with Me_2Cd (Scheme 2).[27]

The molecular structures [Tm$^{Bu^t}$]Cd(O_2CR) (R = C_6H_4-4-Me, C_6H_4-4-F, C_6H_3-3,5-F_2, C_6H_3-2,6-F_2, 9-anthryl, C_3H_6Ph) have been determined by X−ray diffraction, as illustrated in Figures 2−7. Selected bond lengths and angles are summarized in Tables 1 and 2. Carboxylate ligands can bind to a single metal center via bidentate, anisobidentate, or unidentate coordination modes that, by analogy to nitrate ligands,[28−30] can be identified by the magnitude of the difference in M−O bond lengths (Δd) and M−O−C bond angles ($\Delta\theta$), as summarized in Table 3. Adopting this classification, the carboxylate coordination modes in [Tm$^{Bu^t}$]Cd(O_2CR) are identified as bidentate since both (i) the differences in Cd−O bond lengths (0.02−0.25 Å) are less than 0.3 Å and (ii) the differences in O−Cd−C bond angles (0.7°−11.5°) are less than 14° (Table 4). As such, the cadmium centers of each of the [Tm$^{Bu^t}$]Cd(O_2CR) complexes are classified as five-coordinate. Analysis of the compounds listed in the Cambridge Structural Database indicates that the majority

Scheme 1

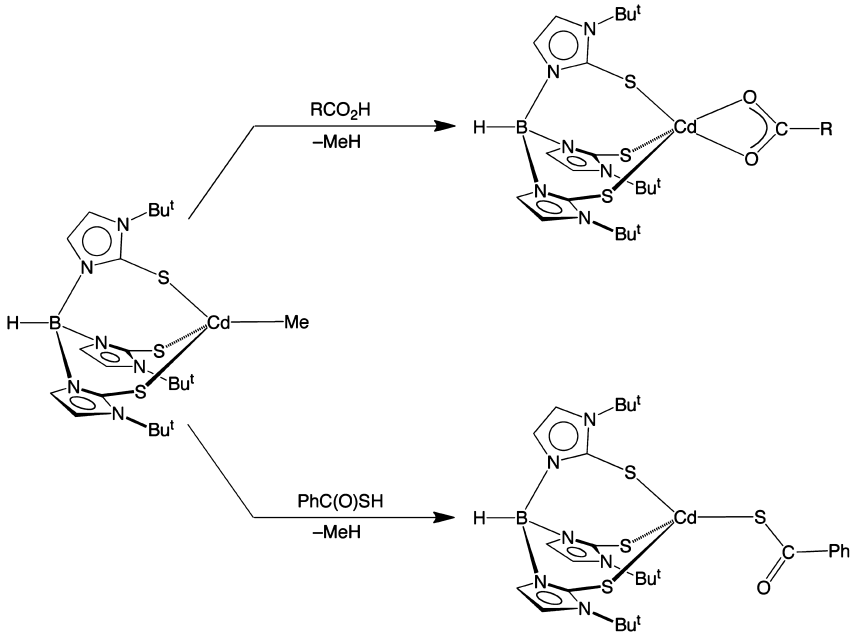

Scheme 2

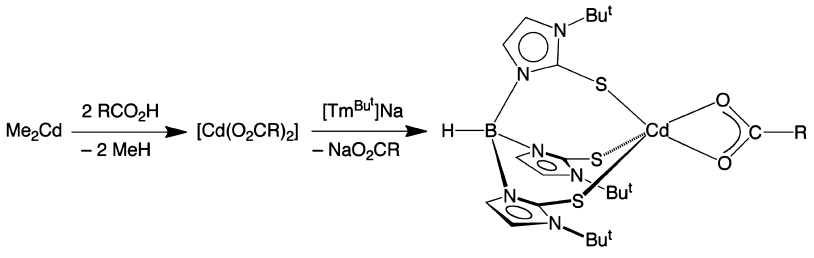

DOI: 10.1021/acs.inorgchem.5b00017
Inorg. Chem. 2015, 54, 3835−3850

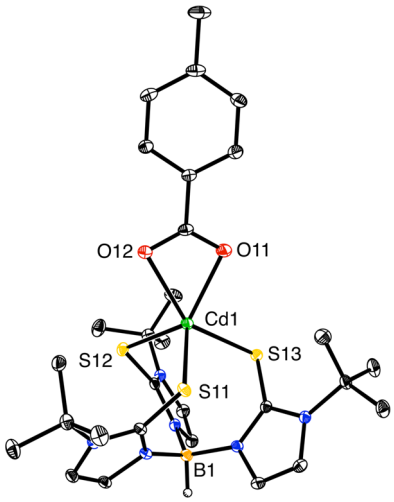

Figure 2. Molecular structure of $[Tm^{Bu^t}]CdO_2C(C_6H_4\text{-}4\text{-}Me)$.

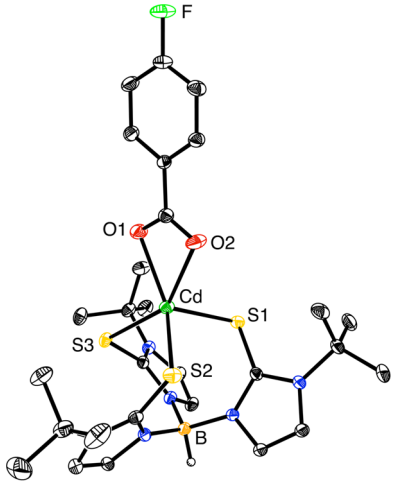

Figure 3. Molecular structure of $[Tm^{Bu^t}]CdO_2C(C_6H_4\text{-}4\text{-}F)$.

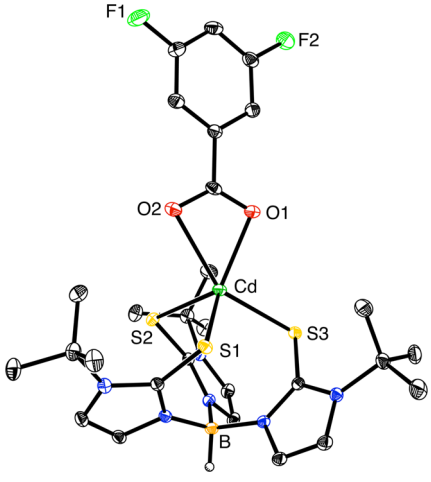

Figure 4. Molecular structure of $[Tm^{Bu^t}]CdO_2C(C_6H_3\text{-}3,5\text{-}F_2)$.

of nonbridging cadmium benzoate compounds are also bidentate (Figures 8 and 9). For example, 66.8% of the compounds have Δd values $\leq$0.3 Å.[31]

Despite the overall similarity in the structures of $[Tm^{Bu^t}]Cd(O_2CR)$, there are subtle differences in the cadmium coordination geometries. For example, the τ_5 five-coordinate geometry

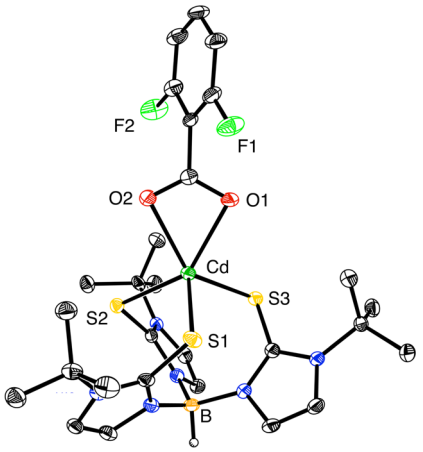

Figure 5. Molecular structure of $[Tm^{Bu^t}]CdO_2C(C_6H_3\text{-}2,6\text{-}F_2)$.

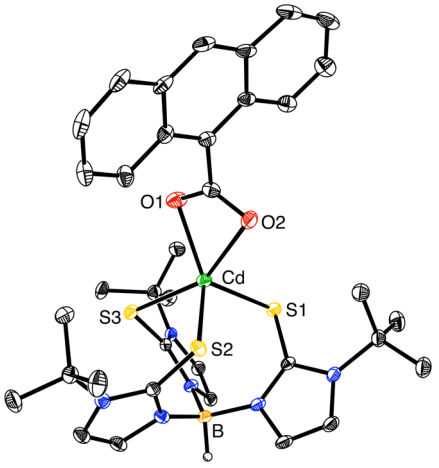

Figure 6. Molecular structure of $[Tm^{Bu^t}]CdO_2C(9\text{-}An)$.

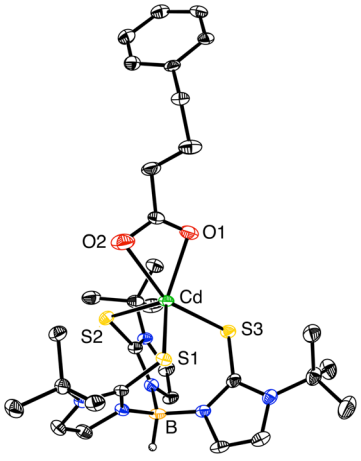

Figure 7. Molecular structure of $[Tm^{Bu^t}]CdO_2C(C_3H_6Ph)$.

indices[32] of $[Tm^{Bu^t}]Cd(O_2CR)$ range from 0.10 (R = C_6H_3-2,6-F_2) to 0.45 (R = C_3H_6Ph), as summarized in Table 4. In view of the fact that an idealized trigonal bipyramid has a τ_5 index of 1.00, while an idealized square pyramid has a τ_5 index of 0.00, it is evident that there is a transition from a square pyramidal geometry to a structure that is midway between these idealized geometries. Interestingly, the structural variation of the cadmium center is linked to the bidenticity of the carboxylate ligand, as

DOI: 10.1021/acs.inorgchem.5b00017
Inorg. Chem. 2015, 54, 3835−3850

Table 1. Selected Bond Lengths for $[Tm^{Bu^t}]Cd(\kappa^2\text{-}O_2CR)$

compound	$d(Cd-S_{X1})$, Å	$d(Cd-S_{X2})$, Å	$d(Cd-S_{X3})$, Å	$d(Cd-O_{X1})$, Å	$d(Cd-O_{X2})$, Å
$[Tm^{Bu^t}]CdO_2C(C_6H_4\text{-}4\text{-}Me)$	2.5225(6), 2.5503(7)	2.5414(7), 2.5544(7)	2.5870(6), 2.5964(7)	2.2645(17), 2.2523(18)	2.4234(16), 2.4750(18)
$[Tm^{Bu^t}]CdO_2C(C_6H_4\text{-}4\text{-}F)$	2.5436(6)	2.5442(7)	2.5609(6)	2.2782(17)	2.4601(17)
$[Tm^{Bu^t}]CdO_2C(C_6H_3\text{-}3,5\text{-}F_2)$	2.5333(4)	2.5351(4)	2.5728(5)	2.2595(13)	2.5069(14)
$[Tm^{Bu^t}]CdO_2C(C_6H_3\text{-}2,6\text{-}F_2)$	2.5321(10)	2.5450(9)	2.5521(10)	2.351(3)	2.371(3)
$[Tm^{Bu^t}]CdO_2C(9\text{-}An)$	2.5226(9)	2.5504(9)	2.5661(9)	2.266(2)	2.465(2)
$[Tm^{Bu^t}]CdO_2C(C_3H_6Ph)$	2.5179(12)	2.5394(13)	2.6095(13)	2.244(4)	2.447(4)

Table 2. Selected Bond Angle Data for $[Tm^{Bu^t}]Cd(O_2CR)$

compound	$Cd-O_{X1}-C$, °	$Cd-O_{X2}-C$, °	$C_{X3}-C_{X2}-C_{X1}-O_{X1}$ Ar–CO_2 torsion angle,[a] °
$[Tm^{Bu^t}]CdO_2C(C_6H_4\text{-}4\text{-}Me)$	94.73(14)	87.49(13)	12.94
	96.68(15)	86.51(15)	10.76
$[Tm^{Bu^t}]CdO_2C(C_6H_4\text{-}4\text{-}F)$	95.35(14)	87.22(14)	2.60
$[Tm^{Bu^t}]CdO_2C(C_6H_3\text{-}3,5\text{-}F_2)$	96.29(11)	84.78(11)	10.28
$[Tm^{Bu^t}]CdO_2C(C_6H_3\text{-}2,6\text{-}F_2)$	91.3(2)	90.6(2)	66.22
$[Tm^{Bu^t}]CdO_2C(9\text{-}An)$	95.1(2)	86.23(19)	68.84
$[Tm^{Bu^t}]CdO_2C(C_3H_6Ph)$	98.1(3)	87.0(3)	

[a]The values listed correspond only to the magnitude of the torsion angle in the range of 0–90°.

Table 3. Criteria for Assigning Carboxylate Coordination Modes[a]

coordination mode	Δd, Å	$\Delta\theta$, °
unidentate	>0.6	>28
anisobidentate	0.3–0.6	14–28
bidentate	<0.3	<14

[a]Adopted from the values for nitrate ligands. See ref 28.

Table 4. Data Pertaining to Carboxylate Coordination Mode and Cd Geometry

compound	Δd, Å[a]	$\Delta\theta$, °[b]	τ_5[c]
$[Tm^{Bu^t}]CdO_2C(C_6H_4\text{-}4\text{-}Me)$	0.16	7.24	0.24
	0.22	10.17	0.44
$[Tm^{Bu^t}]CdO_2C(C_6H_4\text{-}4\text{-}F)$	0.18	8.13	0.28
$[Tm^{Bu^t}]CdO_2C(C_6H_3\text{-}3,5\text{-}F_2)$	0.25	11.51	0.37
$[Tm^{Bu^t}]CdO_2C(C_6H_3\text{-}2,6\text{-}F_2)$	0.02	0.7	0.10
$[Tm^{Bu^t}]CdO_2C(9\text{-}An)$	0.20	8.87	0.40
$[Tm^{Bu^t}]CdO_2C(C_3H_6Ph)$	0.20	11.1	0.45

[a]$\Delta d = d(Cd-O_{X2}) - d(Cd-O_{X1})$. [b]$\Delta\theta = \theta(Cd-O_{X1}-C) - \theta(Cd-O_{X2}-C)$. [c]$\tau_5 = (\beta - \alpha)/60$, where $\beta - \alpha$ is the difference between the two largest angles.

illustrated by the correlation between the τ_5 index and Δd (Figure 11), although it should be noted that there is some scatter in the data. Thus, the transition from a square pyramidal geometry towards a trigonal bipyramidal geometry is accompanied by a general increase in the asymmetry of the carboxylate ligand.

Another noteworthy feature of the arylcarboxylate compounds pertains to the torsion angle between the aryl and carboxylate groups. Specifically, the torsion angle between these groups (Table 2) falls into two classes, i.e., those in which the two groups are close to coplanar (≤15°) and those in which they are closer to orthogonal (≥66°). As would be expected, these torsion angles are dictated by the presence of ortho substituents, such that the two compounds with largest torsion angles are $[Tm^{Bu^t}]CdO_2C(C_6H_3\text{-}2,6\text{-}F_2)$ and $[Tm^{Bu^t}]CdO_2C(9\text{-}An)$, as illustrated in Figures 5 and 6. These torsion angles, however, have little influence on the bidenticity of the carboxylate ligand.

Metal carboxylate $\nu(CO_2)_{asym}$ and $\nu(CO_2)_{sym}$ IR absorptions can be used, in principle, to differentiate between unidentate

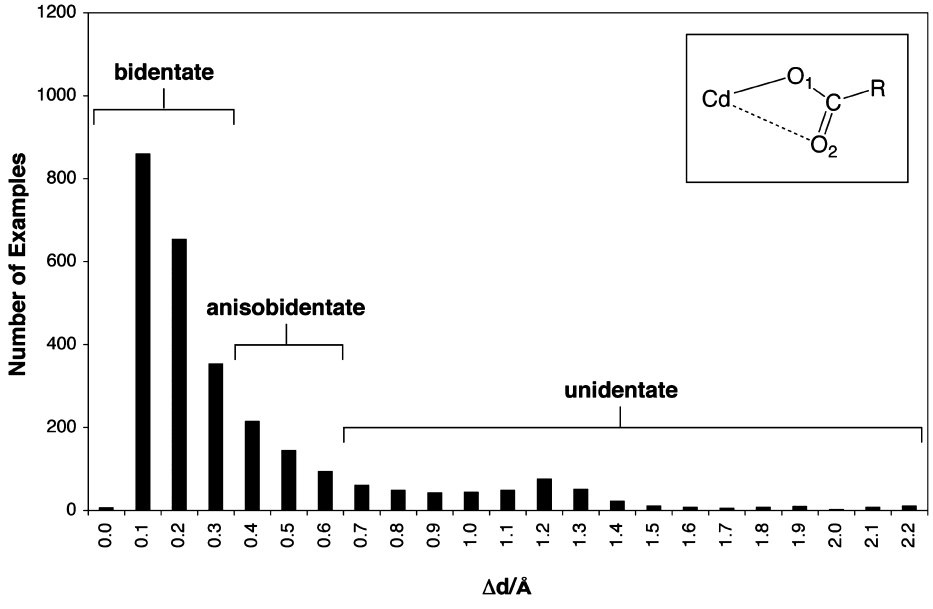

Figure 8. Distribution of Δd, i.e., $d(Cd-O_2) - d(Cd-O_1)$, values for nonbridging benzoate compounds listed in the Cambridge Structural Database. The values on the *x*-axis indicate the maximum value of Δd in the bin.

DOI: 10.1021/acs.inorgchem.5b00017
Inorg. Chem. 2015, 54, 3835–3850

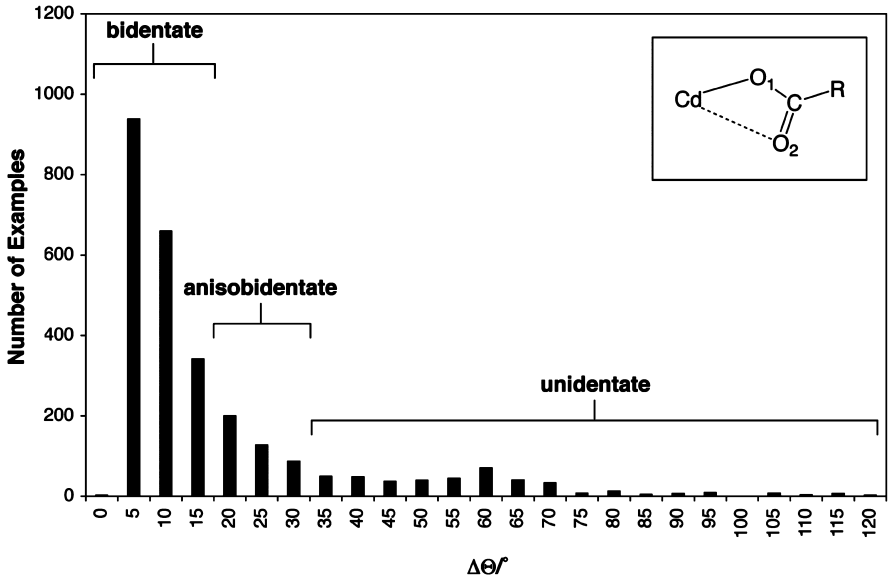

Figure 9. Distribution of $\Delta\theta$ values, i.e., (Cd−O_1−C) − (Cd−O_2−C), for nonbridging benzoate compounds listed in the Cambridge Structural Database. The values on the *x*-axis indicate the maximum value of $\Delta\theta$ in the bin.

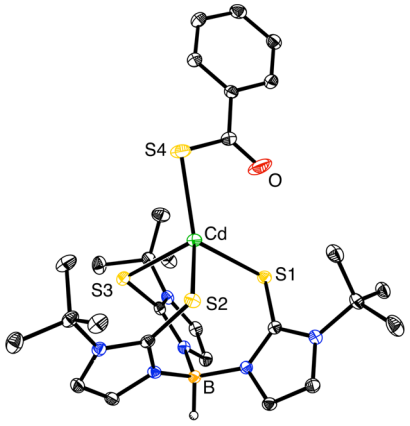

Figure 10. Molecular structure of [Tm^{Bu^t}]Cd[κ^1-SC(O)Ph].

and bidentate coordination modes, although discrimination at the borderlines is not straightforward.[30] In this regard, although $\nu(CO_2)_{sym}$ absorptions for [Tm^{Bu^t}]Cd(O_2CR) cannot be readily identified due to interference by other absorptions, $\nu(CO_2)_{asym}$ can be identified in the region of 1535−1567 cm^{-1}. These values are, nevertheless, consistent with the bidentate coordination modes observed by X-ray diffraction. For example, bidentate coordination modes are usually characterized by $\nu(CO_2)_{asym}$ values that are typically less than 1575 cm^{-1}.[30]

2. Synthesis and Structural Characterization of a Cadmium Thiobenzoate Complex, [Tm^{Bu^t}]Cd[κ^1-SC(O)Ph]. Similar to the carboxylate compounds, the thiobenzoate complex [Tm^{Bu^t}]Cd[κ^1-SC(O)Ph] can be synthesized by treatment of [Tm^{Bu^t}]CdMe with thiobenzoic acid (Scheme 1). [Tm^{Bu^t}]Cd[κ^1-SC(O)Ph] is characterized by an absorption at 1550 cm^{-1} in the IR spectrum that may be assigned to ν(CO), which is in the range observed for other thiocarboxylate compounds.[33−36] For example, Cd[SC(O)Ph]$_2$ is characterized by absorptions at 1580 and 1597 cm^{-1}.[33]

The molecular structure of [Tm^{Bu^t}]Cd[κ^1-SC(O)Ph] has been determined by X-ray diffraction as illustrated in Figure 10. As with carboxylate compounds, thiocarboxylate ligands can adopt a variety of coordination modes, including (i) unidentate and bidentate coordination to a single metal and (ii) several bridging modes.[36,37] In this regard, with respect to coordination of the thiobenzoate ligand, the Cd···O interaction (2.982 Å) is substantially longer than the Cd−S bond (2.478 Å).[38] Thus, whereas the carboxylate ligands in [Tm^{Bu^t}]Cd(κ^2-O_2CR) coordinate in a bidentate manner, it is evident that the thiobenzoate ligand in [Tm^{Bu^t}]Cd[κ^1-SC(O)Ph] coordinates in a S-bound unidentate fashion. As such, the cadmium center adopts a distorted tetrahedral geometry with a τ_4 parameter[39] of 0.80.[40]

In accord with the X-type[41] nature of the Cd−SC(O)Ph interaction in [Tm^{Bu^t}]Cd[κ^1-SC(O)Ph], the Cd−S bond involving the thiobenzoate ligand (2.478 Å) is shorter than the average value for those involving the L_2X[41] [Tm^{Bu^t}] ligand [2.53−2.59 Å, average = 2.56 Å]. A similar trend is also observed for [Tm^{Bu^t}]CdSPh, in which the Cd−SPh bond [2.4595(7)] is shorter than the average Cd−S bond for the [Tm^{Bu^t}] ligand (2.565 Å).[20]

Further comparison of the denticity of the thiobenzoate ligand with other compounds requires consideration of the different covalent radii of oxygen and sulfur. Specifically, whereas the denticity of a carboxylate ligand can be simply ascertained by evaluating the difference in the two M−O bond lengths (Δd), the evaluation of the coordination mode of a thiocarboxylate ligand requires the different covalent radii of oxygen and sulfur to be taken into account when employing the corresponding Δd_{S-O} values, as defined by d(Cd−S) − d(Cd−O). Thus, on the basis that the covalent radius of sulfur (1.05 Å) is 0.39 Å larger than that of oxygen (0.66 Å),[42] Δd_{S-O} values less than 0.39 Å can be considered to be indicative of primary coordination via sulfur. Correspondingly, Δd_{S-O} values greater than 0.39 Å are indicative of primary coordination via oxygen, while a value of 0.39 Å may be classified as a "symmetric" thiocarboxylate complex. Adopting the Δd value of 0.3 Å (Table 3) employed in the classification of nitrate and carboxylate ligands as an upper limit for bidentate coordination of these O_2 donor ligands,[28] a Δd_{S-O} value of 0.69 Å (i.e., 0.39 Å + 0.30 Å) may be established as an upper limit for bidentate thiocarboxylate coordination, in which the primary

DOI: 10.1021/acs.inorgchem.5b00017
Inorg. Chem. 2015, 54, 3835−3850

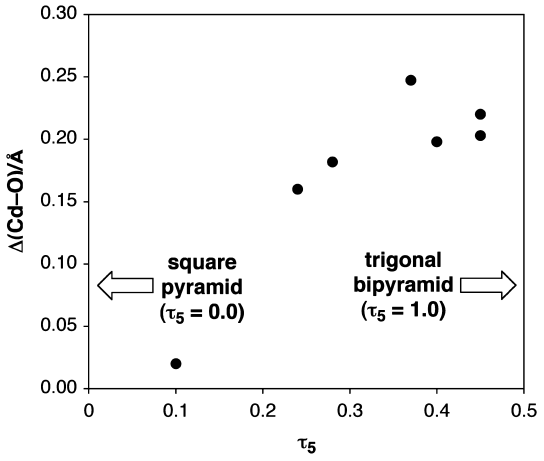

Figure 11. Correlation between the five-coordinate geometry index (τ_5) and the bidenticity (Δd) of the carboxylate ligands in [Tm$^{Bu^t}$]Cd(O$_2$CR) complexes. A trigonal bipyramid has an idealized τ_5 index of 1.00, while an idealized square pyramid has a τ_5 index of 0.00.

Table 5. Classification of Thiocarboxylate Coordination Modes

coordination mode	Δd_{S-O}, Å
S−unidentate	<−0.21
S−anisobidentate	−0.21−0.09
bidentate	0.09−0.69
O−anisobidentate	0.69−0.99
O−unidentate	>0.99

coordination is via oxygen. Correspondingly, a lower limit for bidentate thiocarboxylate coordination corresponds to a Δd_{S-O} value of 0.09 Å (i.e., 0.39 Å − 0.30 Å), in which the primary coordination is via sulfur. Thus, bidentate thiocarboxylate coordination can be identified by values of Δd_{S-O} in the range 0.09−0.69 Å. Similarly, adopting the value of 0.6 Å to differentiate between symmetric bidentate and unidentate coordination modes of carboxylate ligands (Table 3), S-bound unidentate ligands can be classified by values of $\Delta d_{S-O} < -0.21$ Å (i.e., 0.39−0.60 Å), while O-bound unidentate ligands can be classified by values of $\Delta d_{S-O} > 0.99$ Å (i.e., 0.39 Å + 0.60 Å), with anisobidentate variants being characterized by intermediate values (Table 5). On this basis, the Δd_{S-O} value of −0.50 Å for [Tm$^{Bu^t}$]Cd[κ^1-SC(O)Ph] is clearly in accord with the aforementioned unidentate S-bound thiobenzoate classification.

To provide additional context for the Δd_{S-O} value of −0.50 Å for [Tm$^{Bu^t}$]Cd[κ^1-SC(O)Ph], the distribution of values for nonbridging[43] metal thiocarboxylate compounds listed in the Cambridge Structural Database has been analyzed, as summarized in Figures 12−14. Examination of the distribution for all metal thiocarboxylate compounds (Table 6 and Figure 12) indicates that most popular category is S-unidentate (78.8%), followed by S-anisobidentate (10.8%) and bidentate (10.3%). Significantly, there is only one metal thiocarboxylate compound that exhibits an O-unidentate coordination mode, namely, (15-crown-5)-Ca[κ^2-SC(O)Me][κ^1-OC(S)Me],[44] as illustrated by a value of Δd_{S-O} = 2.44 Å.[45]

Cadmium exhibits a distribution that is narrower than observed for all metals (Figure 13), and there is a shift from a preference for S-unidentate coordination for all metals towards S-anisobidentate coordination for cadmium: S-unidentate (11.5%), S-anisobidentate (54.1%), and bidentate (34.4%). A similar distribution is observed for cadmium thiobenzoate compounds, with S-anisobidentate (64.7%) being the most common (Figure 14). Of particular note, none of the previously reported cadmium thiobenzoate compounds possess as much unidentate character as that of [Tm$^{Bu^t}$]Cd[κ^1-SC(O)Ph], for which Δd_{S-O} is −0.50 Å. For example, the closest value to that for [Tm$^{Bu^t}$]Cd[κ^1-SC(O)Ph] is for polymeric {Cd[κ^1-SC(O)Ph]-(μ-4,4′-bipyridine)}$_n$, for which Δd_{S-O} is −0.25 Å.[46] Furthermore, only one metal thiocarboxylate, namely, the mercury

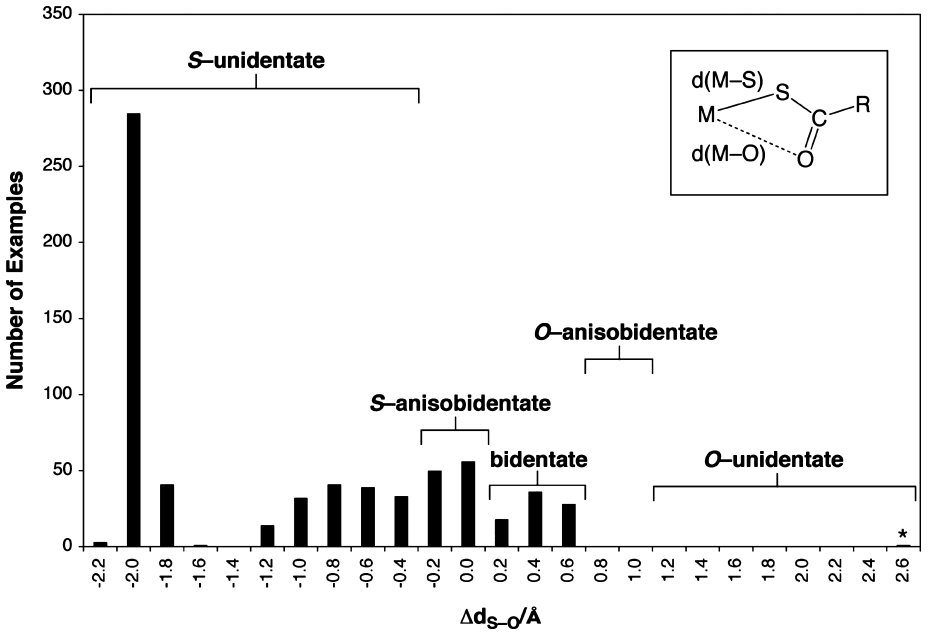

Figure 12. Distribution of metal thiocarboxylate compounds according to the value of Δd_{S-O}, as defined by d(M−S) − d(M−O). The values on the x-axis indicate the maximum value of Δd_{S-O} in the bin. Note that there is only one example of O−unidentate coordination, which is marked with an asterisk.

DOI: 10.1021/acs.inorgchem.5b00017
Inorg. Chem. 2015, 54, 3835−3850

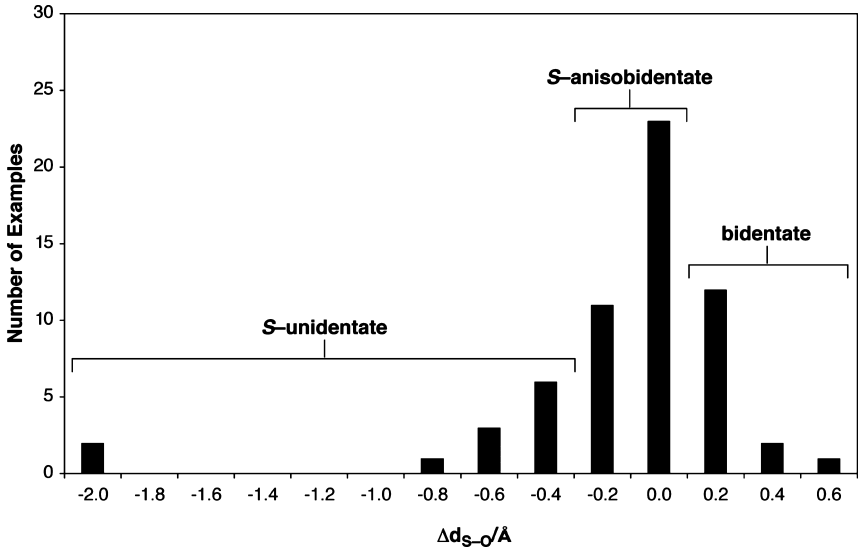

Figure 13. Distribution of cadmium thiocarboxylate compounds according to the value of Δd_{S-O}, as defined by d(Cd−S) − d(Cd−O). The values on the x-axis indicate the maximum value of Δd_{S-O} in the bin.

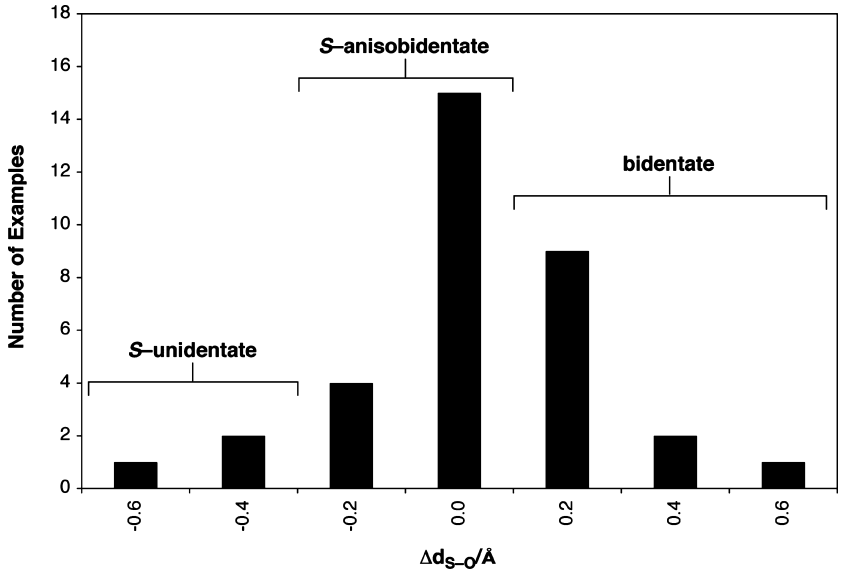

Figure 14. Distribution of cadmium thiobenzoate compounds according to the value of Δd_{S-O}, as defined by d(Cd−S) − d(Cd−O). The values on the x-axis indicate the maximum value of Δd_{S-O} in the bin.

Table 6. Distribution of Metal Thiocarboxylate According to the Value of Δd_{S-O}, as Defined by d(M−S) − d(M−O)

coordination mode	M[SC(O)R] (%)	Cd[SC(O)R] (%)	Cd[SC(O)Ph] (%)
S−unidentate	78.76	34.42	17.65
S−anisobidentate	10.77	54.10	64.71
bidentate	10.32	11.48	17.65
O−anisobidentate	0.00	0.00	0.00
O−unidentate	0.15	0.00	0.00

compound $[Me_4N]\{Hg[SC(O)Ph]\}_3$, has a more negative Δd_{S-O} value (−0.62 Å),[47] i.e., a greater degree of S-unidenticity, than that for $[Tm^{Bu^t}]Cd[\kappa^1$-SC(O)Ph].

While the adoption of S-unidentate, rather than O-unidentate, coordination of thiobenzoate to cadmium in $[Tm^{Bu^t}]Cd[\kappa^1$-SC(O)Ph] may be attributed to hard−soft principles[48] and the thiophilicity of cadmium, the observation that there are no examples of well-defined O-unidentate compounds listed in the Cambridge Structural Database for any metal suggests that this view is overly simplistic. An alternative simple explanation to rationalize both (i) S-unidentate coordination in $[Tm^{Bu^t}]$-$Cd[\kappa^1$-OC(S)Ph] and (ii) the general absence of O-unidentate coordination in the literature, is to recognize that S-unidentate coordination retains a C═O double bond, whereas O-unidentate coordination retains a C═S double bond. Thus, in view of the fact that the combination of a C═O double bond and a C−S single bond is ca. 30 kcal mol^{-1} thermodynamically more favorable than a combination comprising a C═S double bond and a C−O single bond,[49,50] it is evident that coordination of a metal to S would be preferred unless the X−O bond were to be more than 30 kcal mol^{-1} stronger than the corresponding X−S bond.

In support of this suggestion, it is pertinent to note that thiocarboxylic acids exist as a tautomeric mix of thiol and thioxo forms RC(O)SH and RC(S)OH, of which the former are the

DOI: 10.1021/acs.inorgchem.5b00017
Inorg. Chem. 2015, 54, 3835−3850

predominant forms in the solid state and in nonpolar solvents.[50,51] While this observation is difficult to reconcile in terms of hard−soft principles (since hard H^+ preferentially coordinates to the soft sulfur atom of $[RC(O)S]^-$, rather than to the hard oxygen atom), it can be readily reconciled in terms of the differences in C═E and C−E (E = O, S) bond energies,[49,50] given that an O−H bond is not stronger than a corresponding S−H bond by more than 30 kcal mol^{-1}.[52]

3. Carboxylate Ligand Exchange Between [Tm$^{Bu^t}$]Cd(O$_2$CAr) and ArCO$_2$H. Dynamic NMR spectroscopy provides, in principle, a method to investigate exchange of carboxylate groups between the carboxylate [Tm$^{Bu^t}$]Cd(O_2CR) and the carboxylic acid RCO_2H. For example, the ^{1}H NMR spectrum of a mixture of [Tm$^{Bu^t}$]Cd(O_2C-*p*-Tol) and *p*-TolCO_2H at room temperature exhibits exchange-averaged signals for the *para*-tolyl (*p*-Tol) groups, as illustrated for the hydrogen atoms ortho[53] to the carboxyl groups in Figure 15.

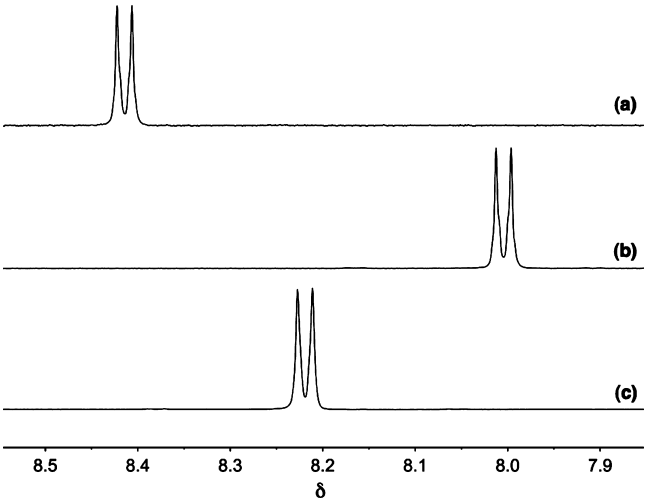

Figure 15. ^{1}H NMR spectrum of (a) [Tm$^{Bu^t}$]Cd(κ^2-O_2C-*p*-Tol), (b) *p*-TolCO_2H, and (c) a mixture of [Tm$^{Bu^t}$]Cd(κ^2-O_2C-*p*-Tol) and *p*-TolCO_2H at room temperature in d_8-toluene. For clarity, only the hydrogen atoms ortho to the carboxyl groups are shown.

While this observation is of considerable significance because it demonstrates that carboxylate exchange is facile, it does not permit a detailed quantification of the exchange. Rather, it merely provides a lower estimate for the exchange rate because the exchange-averaged signal exhibits no line broadening and is in the fast-exchange region.[54] Specifically, since the chemical shift difference between pairs of ortho hydrogens in [Tm$^{Bu^t}$]Cd(O_2C-*p*-Tol) and *p*-TolCO_2H is 0.41 ppm (i.e., $\Delta\nu$ = 205 Hz at 500 MHz), it is evident that the rate constant for site exchange is $>1 \times 10^3$ s^{-1}.[55] Nevertheless, upon cooling, the rate of exchange slows down sufficiently that the exchange-averaged signal broadens (Figure 16). However, at the lowest temperature investigated, the rate is still sufficiently fast that decoalescence is not observed and that the exchange remains in the fast regime, with a single signal. Although rate data may be extracted from these spectra, the situation is complicated by the fact that the chemical shift of the exchange-averaged signal varies significantly as a function of temperature, ranging from 8.22 ppm at room temperature to 8.46 ppm at 188 K. The origin of the temperature dependence of the exchange-averaged signal is that the chemical shifts of both [Tm$^{Bu^t}$]Cd(κ^2-O_2C-*p*-Tol) and *p*-TolCO_2H are also temperature-dependent.

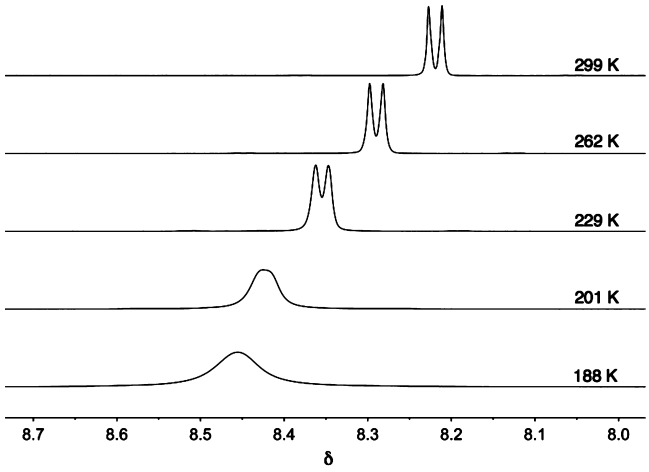

Figure 16. ^{1}H NMR spectrum of a mixture of [Tm$^{Bu^t}$]Cd(κ^2-O_2C-*p*-Tol) and *p*-TolCO_2H as a function of temperature. For clarity, only the hydrogen atoms ortho to the carboxyl groups are shown.

For example, the chemical shift of the ortho hydrogen atoms of [Tm$^{Bu^t}$]Cd(O_2C-*p*-Tol) varies from 8.41 ppm at room temperature to 8.70 ppm at 188 K, while that for *p*-TolCO_2H varies from 8.00 ppm at room temperature to 8.15 at 188 K. Adopting the chemical shift values of 8.70 and 8.15 at 188 K for [Tm$^{Bu^t}$]Cd(O_2C-*p*-Tol) and *p*-TolCO_2H, respectively, the first order rate constant for site exchange is calculated to be 3.0×10^2 s^{-1} (Figure 17).[56]

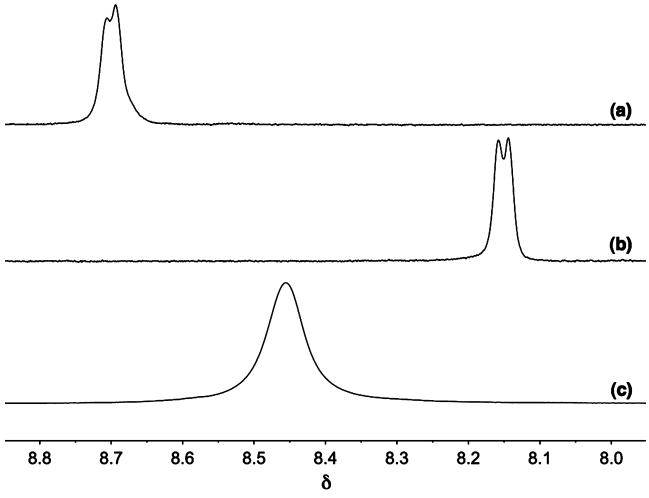

Figure 17. ^{1}H NMR spectrum (500 MHz) of (a) [Tm$^{Bu^t}$]Cd(κ^2-O_2C-*p*-Tol), (b) *p*-TolCO_2H, and (c) a mixture of [Tm$^{Bu^t}$]Cd(κ^2-O_2C-*p*-Tol) and *p*-TolCO_2H at 188 K. For clarity, only the hydrogen atoms ortho to the carboxyl groups are shown. The first-order rate constant for site exchange is 3.0×10^2 s^{-1}.

In view of the fact that it was not possible to observe decoalescence of [Tm$^{Bu^t}$]Cd(O_2C-*p*-Tol) and *p*-TolCO_2H by ^{1}H NMR spectroscopy, our attention turned to the use of ^{19}F NMR spectroscopy to probe exchange between [Tm$^{Bu^t}$]-Cd(O_2CAr^F) and Ar^FCO_2H. Specifically, since the chemical shift range for ^{19}F is much greater than that for the ^{1}H nucleus in typical compounds,[57] ^{19}F NMR spectroscopy provides a means to quantify the kinetics of reactions that are too rapid to be measured by line-shape analysis of the corresponding ^{1}H NMR spectra. For example, while the ^{1}H chemical shifts of the ortho

DOI: 10.1021/acs.inorgchem.5b00017
Inorg. Chem. 2015, 54, 3835−3850

hydrogens[58] of $[Tm^{Bu^t}]Cd(O_2CAr^F)$ (8.34 ppm) and Ar^FCO_2H (7.79 ppm) differ by 0.94 ppm (i.e., 278 Hz at 500 MHz, 11.7 T), the ^{19}F NMR chemical shifts differ by 6.45 ppm (i.e., 3,035 Hz at 470.59 MHz, 11.7 T). As such, ^{19}F NMR spectroscopy is capable of measuring kinetics in this system that are an order of magnitude faster than can be measured by ^1H NMR spectroscopy. Thus, while an exchange-averaged ^{19}F NMR signal is observed for a mixture of $[Tm^{Bu^t}]Cd(O_2CAr^F)$ and Ar^FCO_2H at room temperature (Figure 18), decoalescence into two distinct signals can be achieved at low temperature (Figure 19).[59]

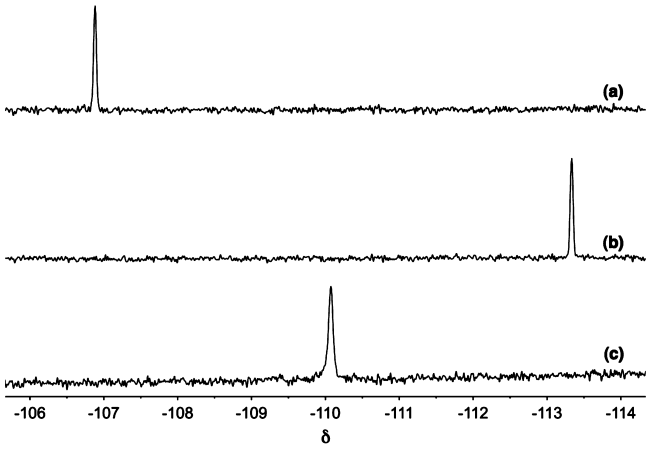

Figure 18. ^{19}F NMR spectra of (a) Ar^FCO_2H, (b) $[Tm^{Bu^t}]Cd(\kappa^2\text{-}O_2CAr^F)$, and (c) a mixture of $[Tm^{Bu^t}]Cd(\kappa^2\text{-}O_2CAr^F)$ and Ar^FCO_2H at room temperature ($Ar^F = C_6H_4\text{-}4\text{-}F$).

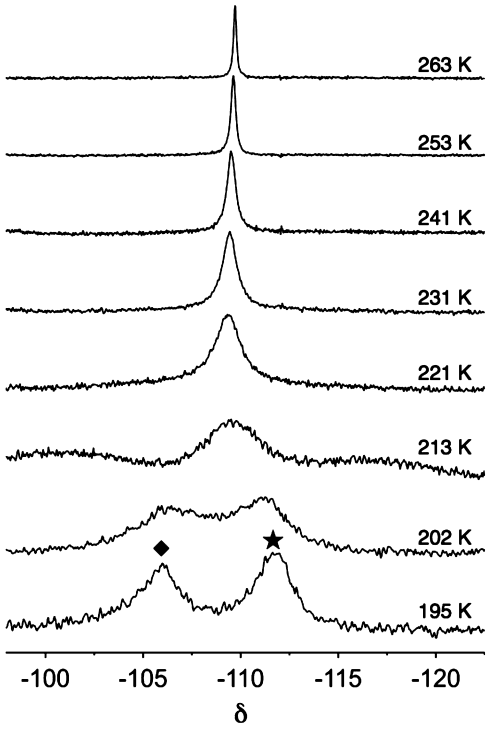

Figure 19. Variable-temperature ^{19}F NMR spectra obtained for a 1:1 mixture of $[Tm^{Bu^t}]Cd(\kappa^2\text{-}O_2CAr^F)$ (★) and Ar^FCO_2H ($Ar^F = 4\text{-}C_6H_4F$) (◆) in C_7D_8.

Although the ability to observe spectra in both the fast- and slow-exchange regimes permits kinetics measurements via line-shape analysis over a large range of temperature (Figure 19 and Table 7),[60] the interpretation of the kinetics data is dependent on the exchange mechanism. In this regard, two simple mechanistic possibilities for the exchange process include (i) an associative pathway in which the carboxylic acid is intimately involved in the rate-determining step and (ii) a dissociative pathway in which the rate-determining step only involves $[Tm^{Bu^t}]Cd(O_2CAr^F)$. To distinguish between these possibilities, the dynamics were studied as a function of the concentration of Ar^FCO_2H at 195 K. For example, if Ar^FCO_2H were not to be involved prior to, or during, the rate-determining step, the line width of $[Tm^{Bu^t}]Cd(O_2CAr^F)$ would not be influenced by the concentration of Ar^FCO_2H; in contrast, the line width of $[Tm^{Bu^t}]Cd(O_2CAr^F)$ would increase if Ar^FCO_2H were to be involved in the rate-determining step. Significantly, the data illustrated in Figure 20 and Table 8 indicate that the exchange rate is dependent on the concentration of Ar^FCO_2H, thereby signaling an associative rather than dissociative pathway.[61]

Table 7. Rate of Carboxylate Exchange between $[Tm^{Bu^t}]Cd(\kappa^2\text{-}O_2CAr^F)$ and Ar^FCO_2H as a Function of Temperature[a]

T, K	rate, Ms^{-1}
263	245
253	150
241	65
231	33
221	24
213	13
202	5
195	2.5

[a]Rates correspond to a solution at room temperature that is composed of $[[Tm^{Bu^t}]Cd(\kappa^2\text{-}O_2CAr^F)]$ (9.1×10^{-4} M) and $[Ar^FCO_2H]_T$ (9.1×10^{-4} M).

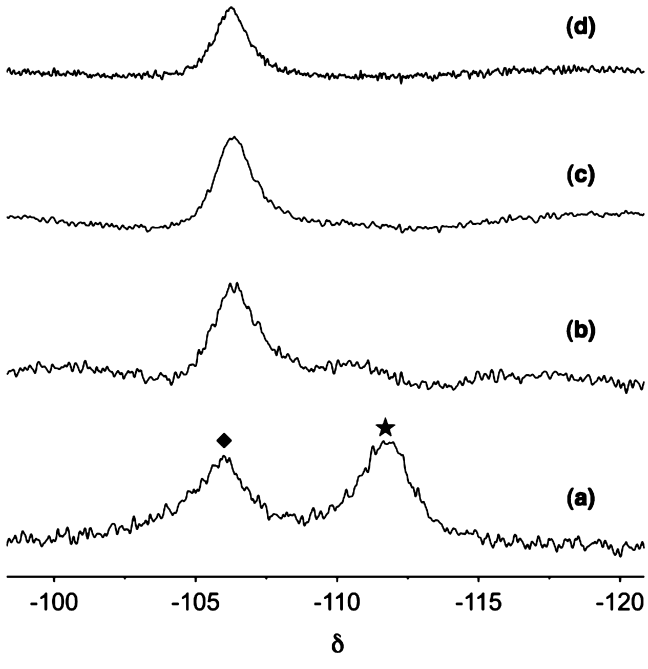

Figure 20. ^{19}F NMR spectra obtained for a mixture of $[Tm^{Bu^t}]Cd(\kappa^2\text{-}O_2CAr^F)$ (★) and Ar^FCO_2H ($Ar^F = 4\text{-}C_6H_4F$) (◆) with different concentrations of the latter in C_7D_8: (a) 1:1, (b) 1:2, (c) 1:3, and (d) 1:4 molar ratios of $[Tm^{Bu^t}]Cd(\kappa^2\text{-}O_2CAr^F)$ and Ar^FCO_2H.

DOI: 10.1021/acs.inorgchem.5b00017
Inorg. Chem. 2015, 54, 3835−3850

Table 8. Rate of Carboxylate Exchange between $[Tm^{Bu^t}]Cd(\kappa^2\text{-}O_2CAr^F)$ and Ar^FCO_2H as a Function of Concentration at 195 K

$[Cd]/M^a$	$[Ar^FCO_2H]_T$, M^b	$[Ar^FCO_2H]_e$, M^c	rate, Ms^{-1}
9.10×10^{-4}	9.10×10^{-4}	1.47×10^{-6}	2.5
9.10×10^{-4}	1.80×10^{-3}	2.07×10^{-6}	6
9.10×10^{-4}	2.70×10^{-3}	2.53×10^{-6}	10
9.10×10^{-4}	3.60×10^{-3}	2.92×10^{-6}	14

^{a}Cd = $[Tm^{Bu^t}]Cd(\kappa^2\text{-}O_2CAr^F)$. ^{b}Total concentration of Ar^FCO_2H as monomer and dimer. ^{c}Total concentration of Ar^FCO_2H as monomer at equilibrium.

Several possibilities exist for an associative mechanism. For example, one possibility is that $[Tm^{Bu^t}]Cd(\kappa^2\text{-}O_2CAr^F)$ and Ar^FCO_2H undergo direct metathesis in which protonation of the carboxylate oxygen is accompanied by formation of a new Cd−O bond, as illustrated in Figure 21.[62] A second possibility is that

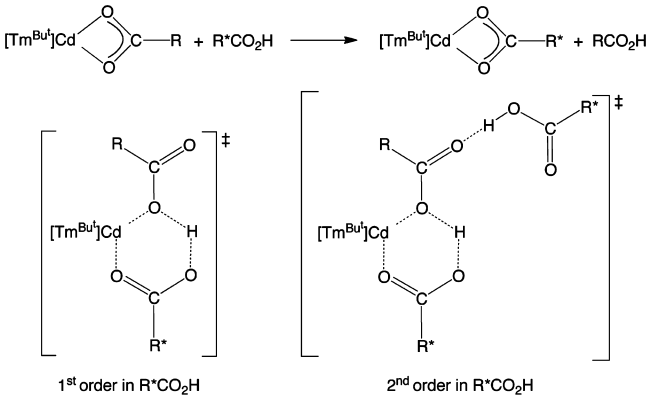

Figure 21. Possible transition states for carboxylate exchange that are consistent with first- and second-order dependence on R^*CO_2H.

$[Tm^{Bu^t}]Cd(O_2CAr^F)$ forms a hydrogen-bonded adduct with Ar^FCO_2H, namely, $[Tm^{Bu^t}]Cd(O_2CAr^F)\cdots HO_2CAr^F$, thereby creating a leaving group, i.e., $[Ar^FCO_2HO_2CAr^F]^-$, which is better than a carboxylate (Figure 21).[62,63] While each of these mechanisms are characterized by rate laws that have different Ar^FCO_2H concentration dependencies, identifying the rate law is complicated by the fact that Ar^FCO_2H exists in equilibrium with the hydrogen-bonded dimer $(Ar^FCO_2H)_2$.[64,65] As such the concentration of Ar^FCO_2H requires consideration of the equilibrium constant for association of the acid (K_{assoc}), which can be estimated as 2.11×10^8 on the basis that (i) the value of K_{assoc} is 1.95×10^4 at 296 K,[64] and (ii) ΔS is −16 e.u.[66] A plot of ln(rate) versus $\ln[Ar^FCO_2H]_e$ may be fit to a straight line with a slope of 2.51 (Figure 22), which is clearly indicative of a nonfirst-order dependence on $[Ar^FCO_2H]_e$. However, on the basis that $[Ar^FCO_2H]_e$ is an estimate, we do not consider it prudent to interpret the slope as providing a precise value for the order of this reaction.

Phenomenologically, the rate can also be expressed in terms of total carboxylic acid concentration $[Ar^FCO_2H]_T$, in which case no distinction is made with respect to the form of the carboxylic acid (monomer or dimer) in solution. For this scenario, a plot of ln(rate) versus $\ln([Ar^FCO_2H]_T)$ may be fit to a straight line with a slope of 1.26. Correspondingly, a plot of rate versus $[[Tm^{Bu^t}]Cd(O_2CAr^F)][Ar^FCO_2H]_T^{1.26}$ through the origin is characterized by a slope of 1.86×10^7 $M^{-1.26}$ s^{-1} for

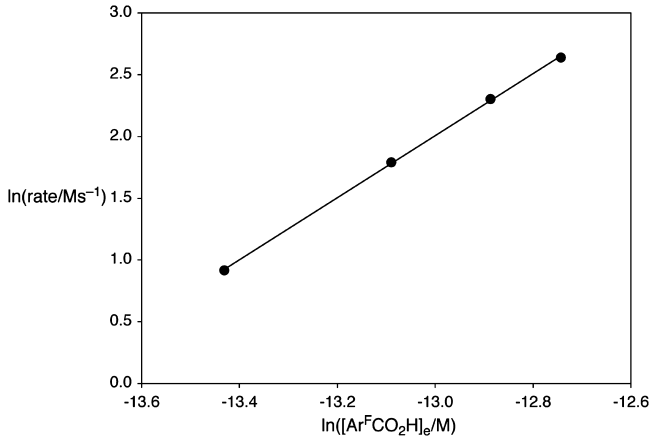

Figure 22. Plot of ln(rate) vs $\ln[Ar^FCO_2H]_e$. A slope of 2.51 is indicative of a reaction that is nonfirst order in $[Ar^FCO_2H]$.

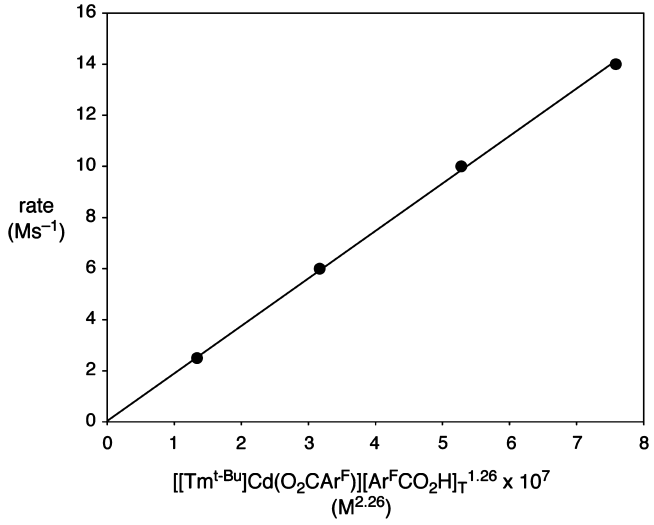

Figure 23. Empirical correlation of carboxylate exchange rate with concentration.

k_{app} (Figure 23). While the empirical expression rate = $k_{app}[[Tm^{Bu^t}]Cd(O_2CAr^F)][Ar^FCO_2H]^{1.26}$ has no mechanistic significance,[67] it is of value in allowing one to estimate an exchange rate as a function of total carboxylic acid concentration, which is of use in predicting reactivity (vide infra).

Although ligand exchange at group 12 metal centers has been investigated in a variety of systems,[68−73] the most relevant comparison is with the tris(pyrazolyl)hydroborato compound $[Tp^{Bu^t}]Cd(O_2CMe)$.[25] In this regard, the observation of an associative mechanism for $[Tm^{Bu^t}]Cd(O_2CAr^F)$ is of interest in view of the fact that the exchange of acetate between the tris(pyrazolyl)hydroborato compound, $[Tp^{Bu^t}]Cd(O_2{}^{13}CMe)$ and $[Na(kryptofix\text{-}221)][Me^{13}CO_2]$, as observed by ^{13}C NMR spectroscopy, was proposed to be dissociative.[25,74] Exchange was also observed between the cyclohexene oxide (CHO) adduct $[Tp^{Bu^t}]Cd(O_2CMe)(CHO)$ and acetic acid, but the mechanism was not addressed;[25] thus, further comparison with $[Tm^{Bu^t}]Cd(O_2CAr^F)$ is not possible.

The observation that ligand exchange involving $[Tm^{Bu^t}]Cd(O_2CAr^F)$ is very facile is of relevance to the fact that cadmium carbonic anhydrase also exhibits a sulfur-rich coordination environment involving cysteine thiolate groups[75] and thus indicates that such an environment is consistent with catalytic turnover.

DOI: 10.1021/acs.inorgchem.5b00017
Inorg. Chem. 2015, 54, 3835−3850

Table 9. Crystal, Intensity Collection, and Refinement Data

	[Tm$^{Bu^t}$]CdO$_2$C(C$_6$H$_4$-4-Me)·0.5MeCN	[Tm$^{Bu^t}$]CdO$_2$C(C$_6$H$_4$-4-F)·2(C$_6$H$_6$)	[Tm$^{Bu^t}$]CdO$_2$C-(C$_6$H$_3$-2,6-F$_2$)	[Tm$^{Bu^t}$]CdO$_2$C(C$_6$H$_3$-3,5-F$_2$)·(Et$_2$O)	[Tm$^{Bu^t}$]CdO$_2$C(C$_3$H$_6$Ph)	[Tm$^{Bu^t}$]CdO$_2$C(9-An)·(C$_6$H$_6$)	[Tm$^{Bu^t}$]CdSC(O)Ph·(C$_6$H$_6$)
lattice	triclinic	monoclinic	monoclinic	monoclinic	monoclinic	monoclinic	triclinic
formula	$C_{60}H_{85}B_2Cd_2N_{13}O_4S_6$	$C_{40}H_{50}BCdFN_6O_2S_3$	$C_{28}H_{37}BCdF_2N_6O_2S_3$	$C_{32}H_{47}BCdF_2N_6O_3S_3$	$C_{31}H_{45}BCdN_6O_2S_3$	$C_{42}H_{49}BCdN_6O_2S_3$	$C_{34}H_{45}BCdN_6OS_4$
formula weight	1491.19	885.25	747.03	821.15	753.12	889.26	805.21
space group	$P\bar{1}$	$P2_1/n$	$P2_1/n$	$P2_1/c$	$P2_1/c$	$P2_1/c$	$P\bar{1}$
a/Å	14.618(2)	12.9391(17)	10.0324(7)	11.0534(7)	19.603(3)	19.0524(17)	10.6011(15)
b/Å	14.677(2)	13.6148(18)	11.0195(8)	18.2044(11)	11.4701(15)	10.7547(9)	11.0621(16)
c/Å	19.035(3)	24.852(4)	30.106(2)	18.9143(11)	15.472(2)	22.323(2)	15.950(2)
α/deg	67.915(2)	90	90	90	90	90	87.140(2)
β/deg	89.636(2)	104.782(2)	90.4850(10)	90.5360(10)	97.844(2)	113.1060(10)	87.683(2)
γ/deg	67.224(2)	90	90	90	90	90	86.158(2)
V/Å^3	3442.8(8)	4233.2(10)	3328.2(4)	3805.8(4)	3446.5(8)	4207.1(6)	1862.6(4)
Z	2	4	4	4	4	4	2
temperature (K)	150(2)	150(2)	150(2)	130(2)	150(2)	150(2)	150(2)
radiation (λ, Å)	0.710 73	0.710 73	0.710 73	0.710 73	0.710 73	0.710 73	0.710 73
ρ (calcd), g cm^{-3}	1.438	1.389	1.491	1.433	1.451	1.404	1.436
μ (Mo Kα), mm^{-1}	0.854	0.709	0.891	0.788	0.853	0.711	0.847
θ max, deg	28.28	30.66	30.61	30.51	30.83	30.68	30.51
no. of data collected	48 367	65 990	53 280	60 420	54 741	67 089	29 077
no. of data used	17 098	13 067	10 252	11 617	10 769	13 021	11 263
no. of parameters	813	500	401	448	410	563	437
R_1 [$I > 2\sigma(I)$]	0.0310	0.0384	0.0526	0.0290	0.0660	0.0526	0.0447
wR_2 [$I > 2\sigma(I)$]	0.0655	0.0768	0.0846	0.0669	0.1035	0.0885	0.0807
R_1 [all data]	0.0470	0.0622	0.1238	0.0394	0.1699	0.1205	0.0749
wR_2 [all data]	0.0723	0.0868	0.1045	0.0728	0.1312	0.1099	0.0909
GOF	1.020	1.033	1.002	1.035	1.012	1.003	1.013
R_{int}	0.0359	0.0555	0.1345	0.0323	0.1691	0.1292	0.0496

DOI: 10.1021/acs.inorgchem.5b00017
Inorg. Chem. 2015, 54, 3835−3850

As an illustration of the facility of ligand exchange, the *pseudo*-first-order rate constant for exchange of $[Tm^{Bu^t}]Cd(O_2CAr^F)$ in a 1 M solution of Ar^FCO_2H[76] is calculated to be $1.86 \times 10^7\ s^{-1}$, which corresponds to a lifetime of 54 ns. For comparison, this lifetime is comparable to the exciton lifetimes in cadmium chalcogenide nanocrystals.[77]

Also of relevance to the present study, the kinetics of carboxylate exchange involving cadmium selenide nanocrystals has likewise been investigated.[7c] In this regard, while the exchange between oleic acid and physisorbed oleic acid is rapid on the NMR time scale, exchange with the bound oleate is slow. Carboxylate ligands may coordinate to a metal center in manifold ways, which include unidentate and bidentate coordination to a single metal center and bridging to two or more metal centers.[30] Bridging coordination modes may be anticipated at the surface of carboxylate-terminated cadmium chalcogenide nanocrystals, which may be less susceptible to exchange.

CONCLUSIONS

In summary, the tris(2-*tert*-butylmercaptoimidazolyl)hydroborato ligand has been used to obtain a series of cadmium carboxylate compounds in a sulfur-rich environment, namely, $[Tm^{Bu^t}]Cd(\kappa^2\text{-}O_2CR)$, which serve as mimics for both cadmium-substituted zinc enzymes and also the surface atoms of cadmium chalcogenide crystals. The facility of ligand exchange processes in this coordination environment has been probed via exchange reactions with the corresponding carboxylic acid, RCO_2H, which indicates that it is rapid on the NMR time scale, even at low temperature. Furthermore, the exchange reaction occurs via an associative rather than dissociative pathway. In addition to carboxylate compounds, the thiocarboxylate derivative $[Tm^{Bu^t}]Cd[\kappa^1\text{-}SC(O)Ph]$ has also been synthesized via the reaction of $[Tm^{Bu^t}]CdMe$ with thiobenzoic acid, and, in contrast to the carboxylate derivatives $[Tm^{Bu^t}]Cd(\kappa^2\text{-}O_2CR)$, the thiocarboxylate ligand binds in a κ^1 manner via only the sulfur atom.

EXPERIMENTAL SECTION

General Considerations. All manipulations were performed using a combination of glovebox, high-vacuum, and Schlenk techniques under a nitrogen atmosphere,[78] except where otherwise stated. Solvents were purified and degassed by standard procedures. NMR solvents were purchased from Cambridge Isotope Laboratories and stored over 3 Å molecular sieves. NMR spectra were measured on Bruker 300 DRX, Bruker 300 DPX, Bruker 400 Avance III, Bruker 400 Cyber-enabled Avance III, and Bruker 500 DMX spectrometers. ^{1}H NMR chemical shifts are reported in ppm relative to $SiMe_4$ ($\delta = 0$) and were referenced internally with respect to the protio solvent impurity (δ = 7.16 for C_6D_5H, 2.08 for C_7D_8, and 7.26 for $CHCl_3$.[79] ^{13}C NMR spectra are reported in ppm relative to $SiMe_4$ ($\delta = 0$) and were referenced internally with respect to the solvent (δ = 128.06 for C_6D_6 and 77.16 for $CDCl_3$).[79] ^{19}F NMR spectra are reported in ppm relative to $CFCl_3$ ($\delta = 0$) and were referenced internally with respect to a C_6F_6 standard ($\delta = -164.9$).[80] Coupling constants are reported in hertz. IR spectra were recorded on a Nicolet 6700 FT-IR Spectrometer, and the data are reported in cm^{-1}. Mass spectra were obtained on a Jeol JMS-HX110H Tandem Double-Focusing Mass Spectrometer with a 10 kV accelerated voltage equipped with fast-atom bombardment (FAB) ion source. Carboxylic acids were obtained from Aldrich, and 4-fluorobenzoic acid was recrystallized from a solution in EtOH/H_2O (50:50) prior to use. Me_2Cd was obtained from Strem and distilled prior to use.

X-ray Structure Determinations. X-ray diffraction data were collected on a Bruker Apex II diffractometer. Crystal data, data collection, and refinement parameters are summarized in Table 9. The structures were solved using direct methods and standard difference map techniques, and they were refined by full-matrix least-squares procedures on F^2 with SHELXTL (Version 2008/4).[81]

Synthesis of $[Tm^{Bu^t}]CdO_2C(C_6H_4\text{-}4\text{-}Me)$. (a) A solution of $[Tm^{Bu^t}]CdMe$[20] (201 mg, 0.33 mmol) in C_6H_6 (ca. 9 mL) was treated with 4-methylbenzoic acid (56 mg, 0.41 mmol), resulting in immediate effervescence. The solution was stirred at room temperature for 1 h, after which period the volatile components were removed in vacuo, and the resulting powder was washed with Et_2O (ca. 2 mL), yielding $[Tm^{Bu^t}]CdO_2C(C_6H_4\text{-}4\text{-}Me)$ as a white solid (157 mg, 65%). Crystals of $[Tm^{Bu^t}]CdO_2C(C_6H_4\text{-}4\text{-}Me)$ suitable for X-ray diffraction were obtained from a solution in MeCN. Anal. Calcd for $[Tm^{Bu^t}]CdO_2C(C_6H_4\text{-}4\text{-}Me)$: C, 48.0%; H, 5.7%; N, 11.6%. Found: C, 47.5%; H, 5.7%; N, 11.3%. ^{1}H NMR (C_6D_6): 1.52 [s, 27H of $HB\{C_2N_2H_2[C(C\underline{H}_3)_3]CS\}_3$], 1.98 [s, 3H of $CdO_2C(4\text{-}C_6H_4C\underline{H}_3)$], 6.42 [d, $^3J_{H-H}$ = 2, 3H of $HB\{C_2N_2\underline{H}_2[C(CH_3)_3]CS\}_3$], 6.68 [d, $^3J_{H-H}$ = 2, 3H of $HB\{C_2N_2\underline{H}_2[C(CH_3)_3]CS\}_3$], 6.95 [d, $^3J_{H-H}$ = 8, 2H of $CdO_2C(4\text{-}C_6\underline{H}_4CH_3)$], 8.60 [d, $^3J_{H-H}$ = 8, 2H of $CdO_2C(4\text{-}C_6\underline{H}_4CH_3)$]. $^{13}C\{^1H\}$ NMR (C_6D_6): 21.4 [1C, $CdO_2C(4\text{-}C_6H_4\underline{C}H_3)$], 28.9 [9C, $HB\{C_2N_2H_2[C(\underline{C}H_3)_3]CS\}_3$], 59.5 [3C, $HB\{C_2N_2H_2[\underline{C}(CH_3)_3]CS\}_3$], 117.0 [3C, $HB\{\underline{C}_2N_2H_2[C(CH_3)_3]CS\}_3$], 122.9 [3C, $HB\{\underline{C}_2N_2H_2[C(CH_3)_3]CS\}_3$], 128.6 [2C, $CdO_2C(4\text{-}\underline{C}_6H_4CH_3)$], 131.5 [2C, $CdO_2C(4\text{-}\underline{C}_6H_4CH_3)$], 132.9 [1C, $CdO_2C(4\text{-}\underline{C}_6H_4CH_3)$] 140.4 [1C, $CdO_2C(4\text{-}\underline{C}_6H_4CH_3)$], 157.6 [t, $^2J_{C-Cd}$ = 9, 3C, $HB\{C_2N_2H_2[C(CH_3)_3]\underline{C}S\}_3$], 175.1 [1C, $CdO_2\underline{C}(4\text{-}C_6H_4CH_3)$]. IR data for $[Tm^{Bu^t}]CdO_2C(C_6H_4\text{-}4\text{-}Me)$ (ATR, cm^{-1}): 3183 (w), 2977 (w), 2923 (w), 2414 (w), 2324 (w), 2162 (w), 2051 (w), 1980 (w), 1608 (m), 1590 (m), 1535 (s), 1482 (w), 1458 (w), 1397 (vs), 1358 (vs), 1293 (m), 1253 (m), 1229 (m), 1195 (s), 1172 (s), 1132 (m), 1119 (m), 1099 (m), 1061 (m), 1047 (m), 1021 (m), 984 (w), 929 (w), 860 (m), 821 (m), 787 (m), 767 (s), 727 (s), 687 (s), 639 (w), 621 (m), 589 (m), 552 (m), 493 (w), 476 (m) FAB-MS: m/z = 591.1 $[M - O_2C(4\text{-}C_6H_4CH_3)]^+$, M = $[Tm^{Bu^t}]CdO_2C(4\text{-}C_6H_4CH_4)$.

(b) A solution of Me_2Cd (36 μL, 0.50 mmol) in C_6H_6 (ca. 4 mL) was treated with $[Tm^{Bu^t}]Na$[15] (251 mg, 0.50 mmol) while stirring. 4-Methylbenzoic acid (137 mg, 1.01 mmol) was added to the reaction mixture, resulting in vigorous effervescence and the immediate formation of a cloudy jellylike precipitate. The mixture was stirred for 45 min and filtered. The volatile components were removed in vacuo to give $[Tm^{Bu^t}]CdO_2C(C_6H_4\text{-}4\text{-}Me)$ as a white solid (150 mg, 41%).

(c) A solution of 4-methylbenzoic acid (1.402 g, 10.30 mmol) in toluene (ca. 5 mL) was stirred and treated slowly with Me_2Cd (370 μL, 5.14 mmol), resulting in the immediate formation of a thick gummy precipitate. Pentane (ca. 20 mL) was added, and the mixture was stirred at room temperature for 30 min to convert the gummy precipitate into a more tractable powder. After this period, the precipitate was isolated by filtration using a frit, washed with pentane (2 × 10 mL), and dried in vacuo to yield $Cd[O_2C(C_6H_4\text{-}4\text{-}Me)]_2$ as a white solid (1.886 g, 96%). A suspension of $Cd[O_2C(C_6H_4\text{-}4\text{-}Me)]_2$ (139 mg, 0.36 mmol) in C_6H_6 (ca. 5 mL) was treated with $[Tm^{Bu^t}]Na$[15] (181 mg, 0.36 mmol) while stirring vigorously, resulting in the formation of a cloudy, jellylike suspension. The mixture was stirred for 30 min, centrifuged (2 × 3 min at 7000 rpm), and filtered. The volatile components were removed from the filtrate in vacuo, and the resulting white powder was washed with Et_2O (ca. 2 × 1 mL), yielding $[Tm^{Bu^t}]CdO_2C(C_6H_4\text{-}4\text{-}Me)$ as a white solid (147 mg, 56%).

Synthesis of $[Tm^{Bu^t}]CdO_2C(C_6H_4\text{-}4\text{-}F)$. (a) A solution of $[Tm^{Bu^t}]CdMe$[20] (528 mg, 0.87 mmol) in C_6H_6 (ca. 40 mL) was treated with 4-fluorobenzoic acid (122 mg, 0.87 mmol), resulting in immediate effervescence. The solution was stirred at room temperature for 45 min, after which period the volatile components were removed in vacuo, yielding $[Tm^{Bu^t}]CdO_2C(C_6H_4\text{-}4\text{-}F)$ as a white solid (534 mg, 84%). Additional purification was achieved by extraction into warm Et_2O (ca. 50 mL), followed by addition of pentane (ca. 10 mL) and reducing the volume in vacuo until a microcrystalline precipitate was deposited. The precipitate was isolated by filtration and dried in vacuo. Crystals suitable for X-ray diffraction were obtained via vapor diffusion of pentane into a solution in benzene. Anal. Calcd for $[Tm^{Bu^t}]CdO_2C(C_6H_4\text{-}4\text{-}F)$: C, 46.1%; H, 5.3%; N, 11.5%. Found: C, 46.5%; H, 5.2%; N, 11.2%. ^{1}H NMR (C_6D_6): 1.52 [s, 27H of $HB\{C_2N_2H_2[C(C\underline{H}_3)_3]CS\}_3$], 6.42 [d, $^3J_{H-H}$ = 2, 3H of $HB\{C_2N_2\underline{H}_2[C(CH_3)_3]CS\}_3$], 6.68 [d, $^3J_{H-H}$ = 2, 3H of $HB\{C_2N_2\underline{H}_2[C(CH_3)_3]CS\}_3$], 6.72 [m, 2H of

DOI: 10.1021/acs.inorgchem.5b00017
Inorg. Chem. 2015, 54, 3835−3850

$CdO_2C(4\text{-}C_6\underline{H}_4F)$], 8.47 [m, 2H of $CdO_2C(4\text{-}C_6\underline{H}_4F)$]. $^{13}C\{^1H\}$ NMR (C_6D_6): 28.9 [9C, $HB\{C_2N_2H_2[C(\underline{C}H_3)_3]CS\}_3$], 59.5 [3C, $HB\{C_2N_2H_2[\underline{C}(CH_3)_3]CS\}_3$], 114.5 [d, $^3J_{C-F}$ = 20, 2C, $CdO_2C(4\text{-}\underline{C}_6H_4F)$], 117.0 [3C, $HB\{\underline{C}_2N_2H_2[C(CH_3)_3]CS\}_3$], 123.0 [3C, $HB\{\underline{C}_2N_2H_2[C(CH_3)_3]CS\}_3$], 131.8 [d, $^4J_{C-F}$ = 3, 1C, $CdO_2C(4\text{-}\underline{C}_6H_4F)$], 133.6 [d, $^2J_{C-F}$ = 9, 2C, $CdO_2C(4\text{-}\underline{C}_6H_4F)$], 157.5 [t, $^2J_{C-Cd}$ = 9, 3C, $HB\{C_2N_2H_2[C(CH_3)_3]\underline{C}S\}_3$], 165.0 [d, $^1J_{C-F}$ = 247, 1C, $CdO_2C(4\text{-}\underline{C}_6H_4F)$], 173.8 [1C, $CdO_2\underline{C}(4\text{-}C_6H_4F)$]. ^{19}F NMR (C_6D_6): −113.2. IR data for $[Tm^{Bu^t}]CdO_2C(C_6H_4\text{-}4\text{-}F)$ (ATR, cm^{-1}): 3177 (w), 3145 (w), 2979 (w), 2920 (w), 2662 (w), 2417 (w), 2324 (w), 2289 (w), 2239 (w), 2162 (w), 2116 (w), 2051 (w), 1981 (w), 1608 (m), 1602 (m), 1546 (m), 1507 (w), 1483 (m), 1458 (w), 1428 (m), 1416 (m), 1397 (s), 1370 (s), 1356 (vs), 1305 (m), 1255 (w), 1223 (s), 1192 (vs), 1175 (s), 1151 (m), 1133 (m), 1087 (m), 1070 (m), 1030 (w), 1016 (w), 989 (w), 929 (w), 864 (m), 822 (m), 785 (s), 757 (s), 735 (s), 724 (s), 685 (s), 621 (vs), 587 (m), 550 (m), 493 (m), 457 (m). FAB-MS: m/z = 591.2 $[M - O_2C(4\text{-}C_6H_4F)]^+$, M = $[Tm^{Bu^t}]CdO_2C(4\text{-}C_6H_4F)$.

(b) A solution of Me_2Cd (36 μL, 0.50 mmol) in C_6H_6 (ca. 4 mL) was treated with $[Tm^{Bu^t}]Na$[15] (247 mg, 0.49 mmol) while stirring. 4-Fluorobenzoic acid (134 mg, 0.95 mmol) was added to the reaction mixture, resulting in vigorous effervescence and the immediate formation of a white jellylike precipitate. The mixture was stirred for 30 min and allowed to settle for 30 min. After this period, the mixture was filtered, and the volatile components were removed in vacuo from the solution to give $[Tm^{Bu^t}]CdO_2C(C_6H_4\text{-}4\text{-}F)$ as a white solid (124 mg, 36%).

Synthesis of $[Tm^{Bu^t}]CdO_2C(C_6H_3\text{-}3,5\text{-}F_2)$. A solution of $[Tm^{Bu^t}]CdMe$[20] (407 mg, 0.67 mmol) in C_6H_6 (ca. 10 mL) was treated with 3,5-fluorobenzoic acid (107 mg, 0.67 mmol), resulting in immediate effervescence. The mixture was stirred at room temperature for 30 min, after which the volatile components were removed in vacuo, and the resulting powder was washed with Et_2O (ca. 2 mL) to yield $[Tm^{Bu^t}]CdO_2C(C_6H_3\text{-}3,5\text{-}F_2)$ as a white solid (0.25 g, 50%). Crystals of $[Tm^{Bu^t}]CdO_2C(C_6H_3\text{-}3,5\text{-}F_2)$ suitable for X-ray diffraction were obtained by cooling a solution in Et_2O. Anal. Calcd for $[Tm^{Bu^t}]CdO_2C(C_6H_3\text{-}3,5\text{-}F_2)\cdot Et_2O$: C, 46.8%; H, 5.8%; N, 10.2%. Found: C, 46.2%; H, 4.9%; N, 9.5%. ^1H NMR (C_6D_6): 1.50 [s, 27H of $HB\{C_2N_2H_2[C(C\underline{H}_3)_3]CS\}_3$], 6.41 [d, $^3J_{H-H}$ = 2, 3H of $HB\{C_2N_2\underline{H}_2[C(CH_3)_3]CS\}_3$], 6.44 [m, 1H of $CdO_2C(3,5\text{-}C_6\underline{H}_3F_2)$], 6.67 [d, $^3J_{H-H}$ = 2, 3H of $HB\{C_2N_2\underline{H}_2[C(CH_3)_3]CS\}_3$], 8.07 [m, 2H of $CdO_2C(3,5\text{-}C_6\underline{H}_3F_2)$]. $^{13}C\{^1H\}$ NMR (C_6D_6): 28.8 [9C, $HB\{C_2N_2H_2[C(\underline{C}H_3)_3]CS\}_3$], 59.5 [3C, $HB\{C_2N_2H_2[\underline{C}(CH_3)_3]CS\}_3$], 105.8 [t, $^2J_{C-F}$ = 26, 1C, $CdO_2C\text{-}(3,5\text{-}\underline{C}_6H_3F_2)$], 113.8 [dd, $^2J_{C-F}$ = 20, $^4J_{C-F}$ = 5, 2C, $CdO_2C(3,5\text{-}\underline{C}_6H_3F_2)$], 117.1 [3C, $HB\{\underline{C}_2N_2H_2[C(CH_3)_3]CS\}_3$], 123.0 [3C, $HB\{\underline{C}_2N_2H_2[C(CH_3)_3]CS\}_3$], 139.5 [t, $^3J_{C-F}$ = 8, 1C, $CdO_2C(3,5\text{-}\underline{C}_6H_3F_2)$], 157.2 [t, $^2J_{C-Cd}$ = 9, 3C, $HB\{C_2N_2H_2[C(CH_3)_3]\underline{C}S\}_3$], 162.9 [dd, $^1J_{C-F}$ = 248, $^3J_{C-F}$ = 11, 2C, $CdO_2C(3,5\text{-}\underline{C}_6H_3F_2)$] 172.2, [t, $^4J_{C-F}$ = 3, 1C, $CdO_2\underline{C}(3,5\text{-}C_6H_3F_2)$]. $^{19}F\{^1H\}$ NMR (C_6D_6): −113.4. IR data for $[Tm^{Bu^t}]CdO_2C(C_6H_4\text{-}3,5\text{-}F_2)$ (ATR, cm^{-1}): 3148 (w), 2978 (w), 2927 (w), 2414 (w), 2235 (w), 2165 (w), 2051 (w), 1982 (w), 1620 (w), 1566 (s), 1482 (w), 1468 (w), 1418 (m), 1393 (s), 1357 (vs), 1305 (m), 1260 (w), 1228 (m), 1193 (vs), 1173 (vs), 1132 (m), 1114 (s), 1071 (m), 1031 (w), 982 (s), 949 (w), 929 (w), 892 (w), 850 (w), 822 (m), 777 (s), 760 (s), 725 (s), 685 (s), 668 (m), 590 (m), 552 (m), 495 (m) 455 (m). FAB-MS: m/z = 591.1 $[M - O_2C(3,5\text{-}C_6H_3F_2)]^+$, M = $[Tm^{Bu^t}]CdO_2C(C_6H_3\text{-}3,5\text{-}F_2)$.

Synthesis of $[Tm^{Bu^t}]CdO_2C(C_6H_3\text{-}2,6\text{-}F_2)$. A solution of $[Tm^{Bu^t}]CdMe$[20] (209 mg, 0.35 mmol) in C_6H_6 (ca. 9 mL) was treated with 2,6-fluorobenzoic acid (55 mg, 0.35 mmol), resulting in immediate effervescence. The mixture was stirred vigorously at room temperature for 1 h, resulting in the formation of a fluffy precipitate. After this, the mixture was allowed to settle for 30 min and then filtered. The volatile components were removed in vacuo, and the resulting powder was washed with Et_2O (ca. 2 × 1 mL) to yield $[Tm^{Bu^t}]CdO_2C(C_6H_3\text{-}2,6\text{-}F_2)$ as a white solid (0.103 g, 40%). Crystals of $[Tm^{Bu^t}]CdO_2C(C_6H_3\text{-}2,6\text{-}F_2)$ suitable for X-ray diffraction were obtained by cooling a solution in Et_2O. Anal. Calcd for $[Tm^{Bu^t}]CdO_2C(C_6H_3\text{-}2,6\text{-}F_2)$: C, 45.0%; H, 5.0%; N, 11.3%. Found: C, 45.1%; H, 4.9%; N, 11.1%. ^1H NMR (C_6D_6): 1.51 [s, 27H of $HB\{C_2N_2H_2[C(C\underline{H}_3)_3]CS\}_3$], 6.40 [d, $^3J_{H-H}$ = 2, 3H of $HB\{C_2N_2\underline{H}_2[C(CH_3)_3]CS\}_3$], 6.45 [m, 1H of $CdO_2C(2,6\text{-}C_6\underline{H}_3F_2)$], 6.66 [d, $^3J_{H-H}$ = 2, 3H of $HB\{C_2N_2\underline{H}_2[C(CH_3)_3]CS\}_3$]. $^{13}C\{^1H\}$ NMR (C_6D_6): 28.8 [9C, $HB\{C_2N_2H_2[C(\underline{C}H_3)_3]CS\}_3$], 59.6 [3C, $HB\{C_2N_2H_2[\underline{C}(CH_3)_3]CS\}_3$], 111.3 [dd, $^2J_{C-F}$ = 20, $^4J_{C-F}$ = 5, 2C, $CdO_2C(2,6\text{-}\underline{C}_6H_3F_2)$], 117.1 [3C, $HB\{\underline{C}_2N_2H_2[C(CH_3)_3]CS\}_3$], 118.1 [t, $^2J_{C-F}$ = 23, 1C, $CdO_2C(2,6\text{-}\underline{C}_6H_3F_2)$], 122.9 [3C, $HB\{\underline{C}_2N_2H_2[C(CH_3)_3]CS\}_3$], 128.8 [t, $^3J_{C-F}$ = 10, 1C, $CdO_2C(2,6\text{-}\underline{C}_6H_3F_2)$], 157.3 [t, $^2J_{C-Cd}$ = 9, 3C, $HB\{C_2N_2H_2[C(CH_3)_3]\underline{C}S\}_3$], 160.5 [dd, $^1J_{C-F}$ = 250, $^3J_{C-F}$ =9, 2C, $CdO_2C(3,5\text{-}\underline{C}_6H_3F_2)$], 169.1 [1C, $CdO_2\underline{C}(2,6\text{-}C_6H_3F_2)$]. ^{19}F NMR (C_6D_6): −113.4. IR data for $[Tm^{Bu^t}]CdO_2C(C_6H_4\text{-}2,6\text{-}F_2)$ (ATR, cm^{-1}): 2982 (w), 2375 (w), 2222 (w), 2165 (w), 2050 (w), 1981 (w), 1622 (m), 1567 (m), 1463 (m), 1417 (m), 1396 (s), 1359 (vs), 1304 (m), 1266 (w), 1231 (m), 1193 (s), 1172 (s), 1128 (m), 1060 (m), 1032 (m), 1004 (s), 929 (w), 854 (m), 820 (m), 755 (m), 731 (s), 688 (s), 587 (s), 552 (m), 521 (m), 494 (m). FAB-MS: m/z = 591.2 $[M - O_2C(2,6\text{-}C_6H_3F_2)]^+$, M = $[Tm^{Bu^t}]CdO_2C(C_6H_3\text{-}2,6\text{-}F_2)$.

Synthesis of $[Tm^{Bu^t}]CdO_2C(C_3H_6Ph)$. A solution of $[Tm^{Bu^t}]CdMe$[20] (215 mg, 0.36 mmol) in C_6H_6 (ca. 9 mL) was treated with 4-phenylbutyric acid (74 mg, 0.45 mmol), resulting in immediate effervescence. The mixture was stirred at room temperature for 1 h. After this period, the volatile components were removed in vacuo, and the resulting powder was washed with Et_2O (ca. 2 mL) to yield $[Tm^{Bu^t}]CdO_2C(C_3H_6Ph)$ as a white solid (145 mg, 54%). Crystals of $[Tm^{Bu^t}]CdO_2C(C_3H_6Ph)$ suitable for X-ray diffraction were obtained from Et_2O. Anal. Calcd for $[Tm^{Bu^t}]CdO_2C(C_3H_6Ph)$: C, 49.4%; H, 6.0%; N, 11.2%. Found: C, 49.7%; H, 5.5%; N, 10.6%. ^1H NMR (C_6D_6): 1.52 [s, 27H of $HB\{C_2N_2H_2[C(C\underline{H}_3)_3]CS\}_3$], 2.12 [q, $^3J_{H-H}$ = 8, 2H of $CdO_2C(C_3\underline{H}_6Ph)$], 2.58 [t, $^3J_{H-H}$ = 7, 2H of $CdO_2C(C_3\underline{H}_6Ph)$], 2.67 [t, $^3J_{H-H}$ = 8, 2H of $CdO_2C(C_3\underline{H}_6Ph)$], 6.42 [d, $^3J_{H-H}$ = 2, 3H of $HB\{C_2N_2\underline{H}_2[C(CH_3)_3]CS\}_3$], 6.67 [d, $^3J_{H-H}$ = 2, 3H of $HB\{C_2N_2\underline{H}_2[C(CH_3)_3]CS\}_3$], 7.04 [m, 1H of $CdO_2C(C_3H_6\underline{Ph})$], 7.14 [m, 4H of $CdO_2C(C_3H_6\underline{Ph})$]. $^{13}C\{^1H\}$ NMR (C_6D_6): 28.9 [9C, $HB\{C_2N_2H_2[C(\underline{C}H_3)_3]CS\}_3$], 29.2[1C, $CdO_2C(\underline{C}_3H_6Ph)$], 35.2 [1C, $CdO_2C(\underline{C}_3H_6Ph)$], 36.2 [1C, $CdO_2C(\underline{C}_3H_6Ph)$], 59.4 [3C, $HB\{C_2N_2H_2[\underline{C}(CH_3)_3]CS\}_3$], 117.0 [3C, $HB\{\underline{C}_2N_2H_2[C(CH_3)_3]CS\}_3$], 122.9 [3C, $HB\{\underline{C}_2N_2H_2[C(CH_3)_3]CS\}_3$], 125.6 [1C, $CdO_2C(C_3H_6\underline{Ph})$], 128.4 [2C, $CdO_2C(C_3H_6\underline{Ph})$], 129.1 [2C, $CdO_2C(C_3H_6\underline{Ph})$], 143.5 [1C, $CdO_2C(C_3H_6\underline{Ph})$], 157.6 [t, $^2J_{C-Cd}$ = 9, 3C, $HB\{C_2N_2H_2[C(CH_3)_3]\text{-}\underline{C}S\}_3$], 181.7 [1C, $CdO_2\underline{C}(C_3H_6Ph)$]. IR data for $[Tm^{Bu^t}]CdO_2C\text{-}(C_3H_6Ph)$ (ATR, cm^{-1}): 2975 (w), 2924 (w), 1550 (s), 1496 (m), 1481 (m), 1453 (m), 1415 (s), 1358 (vs), 1295 (m), 1255 (m), 1228 (m), 1195 (s), 1165 (s), 1119 (m), 1061 (m), 1030 (m), 929 (w), 821 (m), 724 (s), 699 (s), 685 (s), 591 (m), 554 (m), 494 (m). FAB-MS: m/z = 591.2 $[M - O_2C(C_3H_6Ph)]^+$, M = $[Tm^{Bu^t}]CdO_2C(C_3H_6Ph)$.

Synthesis of $[Tm^{Bu^t}]CdO_2C(9\text{-Anthryl})$. A solution of $[Tm^{Bu^t}]CdMe$[20] (144 mg, 0.24 mmol) in C_6H_6 (ca. 9 mL) was treated with 9-anthracenecarboxylic acid (73 mg, 0.33 mmol), resulting in immediate effervescence. The resulting cloudy mixture was stirred vigorously at room temperature for 2.5 h. After this, the volatile components were removed in vacuo, and the resulting powder was washed with Et_2O (ca. 2 mL), yielding $[Tm^{Bu^t}]CdO_2C(9\text{-anthryl})$ as a pale yellow solid (142 mg, 74%). Crystals of $[Tm^{Bu^t}]CdO_2C(9\text{-anthryl})$ suitable for X-ray diffraction were obtained from a solution in benzene. Anal. Calcd for $[Tm^{Bu^t}]CdO_2C(9\text{-anthryl})$: C, 53.3%; H, 5.3%; N, 10.4%. Found: C, 53.3%; H, 4.4%; N, 9.6%. ^1H NMR (C_6D_6): 1.56 [s, 27H of $HB\{C_2N_2H_2[C(C\underline{H}_3)_3]CS\}_3$], 6.45 [d, $^3J_{H-H}$ = 2, 3H of $HB\{C_2N_2\underline{H}_2[C(CH_3)_3]CS\}_3$], 6.72 [d, $^3J_{H-H}$ = 2, 3H of $HB\{C_2N_2\underline{H}_2[C(CH_3)_3]CS\}_3$], 7.21 [t, $^3J_{H-H}$ = 8, 2H of $CdO_2C(C_{14}\underline{H}_9)$], 7.29 [t, $^3J_{H-H}$ = 7, 2H of $CdO_2C(C_{14}\underline{H}_9)$], 7.74 [d, $^3J_{H-H}$ = 7, 2H of $CdO_2C(C_{14}\underline{H}_9)$], 8.09 [s, 1H of $CdO_2C(C_{14}\underline{H}_9)$], 8.88 [d, $^3J_{H-H}$ = 9, 2H of $CdO_2C(C_{14}\underline{H}_9)$]. $^{13}C\{^1H\}$ NMR (C_6D_6): 28.9 [9C, $HB\{C_2N_2H_2[C(\underline{C}H_3)_3]CS\}_3$], 59.6 [3C, $HB\{C_2N_2H_2[\underline{C}(CH_3)_3]CS\}_3$], 117.1 [3C, $HB\{\underline{C}_2N_2H_2[C(CH_3)_3]CS\}_3$], 123.1 [3C, $HB\{\underline{C}_2N_2H_2[C(CH_3)_3]CS\}_3$], 125.1 [2C, $CdO_2C(\underline{C}_{14}H_9)$], 125.3 [2C, $CdO_2C(\underline{C}_{14}H_9)$], 126.5 [1C, $CdO_2C(\underline{C}_{14}H_9)$], 128.1 [4C, $CdO_2C(\underline{C}_{14}H_9)$], 128.7 [2C, $CdO_2C(\underline{C}_{14}H_9)$], 128.8 [2C, $CdO_2C(\underline{C}_{14}H_9)$], 132.1 [1C, $CdO_2C\text{-}(\underline{C}_{14}H_9)$], 157.4 [t, $^2J_{C-Cd}$ = 9, 3C, $HB\{C_2N_2H_2[C(CH_3)_3]\underline{C}S\}_3$], 177.5 [1C, $CdO_2\underline{C}(C_3H_6Ph)$]. IR data for $[Tm^{Bu^t}]CdO_2C(9\text{-anthryl})$

DOI: 10.1021/acs.inorgchem.5b00017
Inorg. Chem. 2015, 54, 3835−3850

(ATR, cm^{-1}): 3185 (w), 2969 (w), 2918 (w), 2411 (w), 2324 (w), 2162 (w), 2051 (w), 1981 (w), 1552 (s), 1483 (m), 1416 (s), 1395 (m), 1359 (vs) 1317 (s), 1276 (m), 1229 (m), 1192 (s), 1172 (s), 1131 (m), 1061 (w), 1015 (w), 956 (w), 928 (w), 881 (m), 868 (m), 845 (m), 821 (m), 796 (w), 777 (s), 759 (s), 730 (vs), 721 (s), 689 (s), 669 (m), 639 (m), 588 (m), 555 (m), 527 (m), 494 (m), 479 (m). FAB-MS: m/z = 591.2 $[M - O_2C(C_{14}H_9)]^+$, M = $[Tm^{Bu^t}]CdO_2C(C_{14}H_9)$.

Synthesis of $[Tm^{Bu^t}]CdO_2C(C_{13}H_{27})$. A solution of $[Tm^{Bu^t}]CdMe$[20] (105 mg, 0.17 mmol) in C_6H_6 (ca. 9 mL) was treated with tetradecanoic (myristic) acid (40 mg, 0.18 mmol), resulting in immediate effervescence. The mixture was stirred vigorously at room temperature for 1 h. After this period, the volatile components were removed in vacuo, and the resulting powder was washed with a mixture of Et_2O (ca. 0.5 mL) and pentane (ca. 2 mL), yielding $[Tm^{Bu^t}]CdO_2C(C_{13}H_{27})$ as a white solid (100 mg, 71%). Anal. Calcd for $[Tm^{Bu^t}]CdO_2C(C_{13}H_{27})$: C, 51.4%; H, 7.5%; N, 10.3%. Found: C, 51.2%; H, 7.7%; N, 9.7%. ^1H NMR (C_6D_6): 0.92 [t, $^3J_{H-H}$ = 7, 3H of $CdO_2C(C_{13}\underline{H}_{27})$], 1.28 [m, 18H of $CdO_2C(C_{13}\underline{H}_{27})$], 1.39 [m, 2H of $CdO_2C(C_{13}\underline{H}_{27})$], 1.53 [s, 27H of $HB\{C_2N_2H_2[C(C\underline{H}_3)_3]CS\}_3$], 1.89 [q, $^3J_{H-H}$ = 7, 2H of $CdO_2C(C_{13}\underline{H}_{27})$], 2.60 [t, $^3J_{H-H}$ = 7, 2H of $CdO_2C(C_{13}\underline{H}_{27})$], 6.40 [d, $^3J_{H-H}$ = 2, 3H of $HB\{C_2N_2\underline{H}_2[C(CH_3)_3]CS\}_3$], 6.68 [d, $^3J_{H-H}$ = 2, 3H of $HB\{C_2N_2\underline{H}_2[C(CH_3)_3]CS\}_3$]. $^{13}C\{^1H\}$ NMR (C_6D_6): 14.4 [1C, $CdO_2C(\underline{C}_{13}H_{27})$], 23.1 [1C, $CdO_2C(\underline{C}_{13}H_{27})$], 27.2 [1C, $CdO_2C(\underline{C}_{13}H_{27})$], 28.6 [1C, $CdO_2C(\underline{C}_{13}H_{27})$], 28.9 [9C, $HB\{C_2N_2H_2[C(\underline{C}H_3)_3]CS\}_3$], 29.9 [1C, $CdO_2C(\underline{C}_{13}H_{27})$], 30.1 [1C, $CdO_2C(\underline{C}_{13}H_{27})$], 30.2 [1C, $CdO_2C(\underline{C}_{13}H_{27})$], 30.2 [1C, $CdO_2C(\underline{C}_{13}H_{27})$], 32.4 [1C, $CdO_2C(\underline{C}_{13}H_{27})$], 35.8 [1C, $CdO_2C(\underline{C}_{13}H_{27})$], 59.4 [3C, $HB\{C_2N_2H_2[\underline{C}(CH_3)_3]CS\}_3$], 116.9 [3C, $HB\{\underline{C}_2N_2H_2[C(CH_3)_3]CS\}_3$], 122.9 [3C, $HB\{\underline{C}_2N_2H_2[C(CH_3)_3]CS\}_3$], 157.7 [3C, $HB\{C_2N_2H_2[C(CH_3)_3]\underline{C}S\}_3$], 181.5 [1C, $CdO_2\underline{C}(C_3H_{27})$]. IR data for $[Tm^{Bu^t}]CdO_2C(C_{13}H_{27})$ (ATR, cm^{-1}): 3189 (w), 3150 (w), 2920 (m), 2851 (m), 2322 (w), 2172 (w), 2056 (w), 1983 (w), 1736 (w), 1544 (m), 1470 (m), 1417 (m), 1398 (m), 1358 (vs), 1302 (m), 1264 (w), 1232 (m), 1196 (s), 1172 (s), 1132 (m), 1101 (m), 1071 (m), 1031 (w), 929 (w), 822 (m), 777 (m), 758 (m), 725 (m), 686 (m), 646 (w), 591 (w), 546 (w), 494 (w), 468 (w). FAB-MS: m/z = 591.2 $[M - O_2C(C_{13}H_{27})]^+$, M = $[Tm^{Bu^t}]CdO_2C(C_{13}H_{27})$.

Synthesis of $[Tm^{Bu^t}]CdSC(O)Ph$. A solution of $[Tm^{Bu^t}]CdMe$[20] (201 mg, 0.33 mmol) in C_6H_6 (ca. 9 mL) was treated with thiobenzoic acid (48 μL, 0.41 mmol), resulting in immediate effervescence. The mixture was stirred at room temperature for 45 min. After this period, the volatile components were removed in vacuo, and the resulting powder was washed with Et_2O (ca. 2 × 1 mL) to yield $[Tm^{Bu^t}]CdSC(O)Ph$ as a pale yellow solid (159 mg, 66%). Crystals of $[Tm^{Bu^t}]CdSC(O)Ph$ suitable for X-ray diffraction were obtained via vapor diffusion of pentane into a solution in benzene. Anal. Calcd for $[Tm^{Bu^t}]CdSC(O)Ph$: C, 46.3%; H, 5.4%; N, 11.6%. Found: C, 47.0%; H, 5.2%; N, 11.4%. ^1H NMR (C_6D_6): 1.52 [s, 27H of $HB\{C_2N_2H_2[C(C\underline{H}_3)_3]CS\}_3$], 6.44 [d, $^3J_{H-H}$ = 2, 3H of $HB\{C_2N_2\underline{H}_2[C(CH_3)_3]CS\}_3$], 6.69 [d, $^3J_{H-H}$ = 2, 3H of $HB\{C_2N_2\underline{H}_2[C(CH_3)_3]CS\}_3$], 7.05 [m, 3H of $CdSC(O)\underline{Ph}$], 8.57 [m, 2H of $CdSC(O)\underline{Ph}$]. $^{13}C\{^1H\}$ NMR (C_6D_6): 28.9 [9C, $HB\{C_2N_2H_2[C(\underline{C}H_3)_3]CS\}_3$], 59.5 [3C, $HB\{C_2N_2H_2[\underline{C}(CH_3)_3]CS\}_3$], 117.0 [3C, $HB\{\underline{C}_2N_2H_2[C(CH_3)_3]CS\}_3$], 122.9 [3C, $HB\{\underline{C}_2N_2H_2[C(CH_3)_3]CS\}_3$], 128.1 [1C, $CdSC(O)\underline{Ph}$], 129.6 [2C, $CdSC(O)\underline{Ph}$], 131.3 [2C, $CdSC(O)\underline{Ph}$], 141.6 [1C, $CdSC(O)\underline{Ph}$], 157.7 [t, $^2J_{C-Cd}$ = 8, 3C, $HB\{C_2N_2H_2[C(CH_3)_3]\underline{C}S\}_3$], 203.7 [1C, $CdS\underline{C}(O)Ph$]. IR data for $[Tm^{Bu^t}]CdSC(O)Ph$ (ATR, cm^{-1}): 3136 (w), 3055 (w), 2966 (w), 2928 (w), 2658 (w), 2409 (w), 2324 (w), 2233 (w), 2167 (w), 2051 (w), 1980 (w), 1587 (m), 1559 (m), 1483 (w), 1445 (w), 1427 (m), 1417 (s), 1396 (m), 1358 (vs), 1304 (m), 1254 (w), 1229 (m), 1192 (vs), 1175 (vs), 1133 (m), 1070 (m), 1062 (m), 1025 (m), 1000 (w), 986 (w), 928 (s), 856 (w), 822 (m), 781 (m), 759 (s), 743 (s), 724 (vs), 692 (vs), 685 (vs), 668 (m), 653 (s), 617 (w), 588 (m), 552 (m), 495 (m), 455 (m). FAB-MS: m/z = 589.2 $[M - SC(O)Ph]^+$, M = $[Tm^{Bu^t}]CdSC(O)Ph$.

Kinetics of Carboxylate Ligand Exchange. (a) Solutions comprising mixtures of $[Tm^{Bu^t}]CdO_2C(C_6H_4$-4-F) and 4-fluorobenzoic acid with known concentration were prepared from stock solutions of the individual compounds in C_7D_8. Specifically, an 8.9 × 10^{-3} M stock solution of $[Tm^{Bu^t}]CdO_2C(C_6H_4$-4-F) was prepared by dissolving finely ground $[Tm^{Bu^t}]CdO_2C(4\text{-}C_6H_4F)$ (32.4 mg, 0.0443 mmol) in C_7D_8 (5 mL) in a volumetric flask, while a 2.8 × 10^{-2} M stock solution of 4-fluorobenzoic acid was prepared by dissolving finely ground 4-fluorobenzoic acid (19.6 mg, 0.140 mmol) in C_7D_8 (5 mL) in a volumetric flask. NMR samples were prepared by combining the appropriate amounts of the above solutions, addition of C_6F_6 (1 μL) as an internal standard, and diluting with C_7D_8 to a volume of 1.00 mL volumetric flask. The temperature of the NMR spectrometer probe was calibrated via the use of a methanol calibration standard,[82] and the rates of exchange were measured by using gNMR,[60] from which the derived rate constants were obtained.

(b) A 1:1 0.027 M mixture of $[Tm^{Bu^t}]Cd(O_2C$-p-Tol) (10.7 mg, 0.0148 mmol) and p-$TolCO_2H$ (2.0 mg, 0.0148 mmol) was prepared by addition of C_7D_8 (0.55 mL) to both compounds and transferred to an NMR tube equipped with a J. Young valve. The temperature of the NMR spectrometer probe was calibrated via the use of a methanol calibration standard,[82] and the rates of exchange were measured by using gNMR.[60]

■ ASSOCIATED CONTENT

Ⓢ Supporting Information

CIF files. This material is available free of charge via the Internet at http://pubs.acs.org.

■ AUTHOR INFORMATION

Corresponding Authors

*E-mail: jso2115@columbia.edu. (J.S.O.)
*E-mail: parkin@columbia.edu. (G.P.)

Notes

The authors declare no competing financial interest.

■ ACKNOWLEDGMENTS

Dr. J. Decatur and M. Appel are thanked for assistance with the ^{19}F NMR spectroscopic experiments, and P. Budzelaar is thanked for advice concerning the use of gNMR. Research reported in this publication was supported by the National Institute of General Medical Sciences of the National Institutes of Health under Award No. R01GM046502 (G.P.). The content is solely the responsibility of the authors and does not necessarily represent the official views of the National Institutes of Health. NMR kinetics measurements were supported by the Department of Energy under Grant No. DE-SC0006410 (J.S.O.).

■ REFERENCES

(1) Friedman, R. *Dalton Trans.* **2014**, *43*, 2878−2887.
(2) (a) Zillner, E.; Fengler, S.; Niyamakom, P.; Rauscher, F.; Köhler, K.; Dittrich, T. *J. Phys. Chem. C* **2012**, *116*, 16747−16754. (b) Liu, F.; Zhu, J.; Wei, J.; Li, Y.; Hu, L.; Huang, Y.; Takuya, O.; Shen, Q.; Toyoda, T.; Zhang, B.; Yao, J.; Dai, S. *J. Phys. Chem. C* **2014**, *118*, 214−222.
(3) (a) Rosenthal, S. J.; McBride, J.; Pennycook, S. J.; Feldman, L. C. *Surf. Sci. Rep.* **2007**, *62*, 111−157. (b) Talapin, D. V.; Lee, J.-S.; Kovalenko, M. V.; Shevchenko, E. V. *Chem. Rev.* **2010**, *110*, 389−458. (c) Kovtun, O.; Arzeta-Ferrer, X.; Rosenthal, S. J. *Nanoscale* **2013**, *5*, 12072−12081. (d) Bera, D.; Qian, L.; Tseng, T. K.; Holloway, P. H. *Materials* **2010**, *3*, 2260−2345. (e) Freitas, J. N.; Goncalves, A. S.; Nogueira, A. F. *Nanoscale* **2014**, *6*, 6371−6397. (f) Mehta, V. N.; Kailasa, S. K.; Wu, H.-F. *J. Nanosci. Nanotechnol.* **2014**, *14*, 447−459. (g) Valizadeh, A.; Mikaeili, H.; Samiei, M.; Farkhani, S. M.; Zarghami, N.; Kouhi, M.; Akbarzadeh, A.; Davaran, S. *Nanoscale Res. Lett.* **2012**, *7*, 480. (h) Rogach, A. L.; Gaponik, N.; Lupton, J. M.; Bertoni, C.; Gallardo, D. E.; Dunn, S.; Pira, N. L.; Paderi, M.; Repetto, P.; Romanov, S. G.; O'Dwyer, C.; Torres, C. M. S.; Eychmuller, A. *Angew. Chem., Int. Ed.* **2008**, *47*, 6538−6549. (i) Rosenthal, S. J.; Chang, J. C.; Kovtun, O.; McBride, J. R.; Tomlinson, I. D. *Chem. Biol.* **2011**, *18*, 10−24. (j) Tang, J.; Sargent, E. H. *Adv. Mater.* **2011**, *23*, 12−29.

DOI: 10.1021/acs.inorgchem.5b00017
Inorg. Chem. 2015, 54, 3835−3850

(4) Burda, C.; Chen, X.; Narayanan, R.; El-Sayed, M. *Chem. Rev.* **2005**, *105*, 1025−1102.
(5) (a) Guyot-Sionnest, P.; Wehrenberg, B.; Yu, D. *J. Chem. Phys.* **2005**, *123*, 074709. (b) Pandey, A.; Guyot-Sionnest, P. *Science* **2008**, *322*, 929−932.
(6) Tang, J.; Kemp, K. W.; Hoogland, S.; Jeong, K. S.; Liu, H.; Levina, L.; Furukawa, M.; Wang, X.; Debnath, R.; Cha, D.; Chou, K. W.; Fischer, A.; Amassian, A.; Asbury, J. B.; Sargent, E. H. *Nat. Mater.* **2011**, *10*, 765−771.
(7) (a) Owen, J. S.; Chan, E. M.; Liu, H.; Alivisatos, A. P. *J. Am. Chem. Soc.* **2010**, *132*, 18206−18213. (b) Hendricks, M. P.; Cossairt, B. M.; Owen, J. S. *ACS Nano* **2012**, *6*, 10054−10062. (c) Fritzinger, B.; Capek, R. K.; Lambert, K.; Martins, J. C.; Hens, Z. *J. Am. Chem. Soc.* **2010**, *132*, 10195−10201.
(8) (a) Feng, Y.; Xing, S.; Xu, J.; Wang, H.; Lim, J. W.; Chen, H. *Dalton Trans.* **2010**, *39*, 349−351. (b) Ji, X.; Copenhaver, D.; Sichmeller, C.; Peng, X. *J. Am. Chem. Soc.* **2008**, *130*, 5726−5735. (c) Hassinen, A.; Moreels, I.; de Mello Donegá, C.; Martins, J. C.; Hens, Z. *J. Phys. Chem. Lett.* **2010**, *1*, 2577−2581. (d) Fritzinger, B.; Moreels, I.; Lommens, P.; Koole, R.; Hens, Z.; Martins, J. C. *J. Am. Chem. Soc.* **2009**, *131*, 3024−3032. (e) von Holt, B.; Kudera, S.; Weiss, A.; Schrader, T. E.; Mana, L.; Parak, W. J.; Braun, M. *J. Mater. Chem.* **2008**, *18*, 2728−2732. (f) Webber, D. H.; Brutchey, R. L. *J. Am. Chem. Soc.* **2012**, *134*, 1085−1092. (g) Koole, R.; Schapotschnikow, P.; Donega, C. D.; Vlugt, T. J. H.; Meijerink, A. *ACS Nano* **2008**, *2*, 1703−1714.
(9) (a) Owen, J. S.; Park, J.; Trudeau, P.-E.; Alivisatos, a P. *J. Am. Chem. Soc.* **2008**, *130*, 12279−12281. (b) Schapotschnikow, P.; Hommersom, B.; Vlugt, T. J. H. *J. Phys. Chem. C* **2009**, *113*, 12690−12698.
(10) Vittal, J. J.; Ng, M. T. *Acc. Chem. Res.* **2006**, *39*, 869−877.
(11) (a) Chaturyedi, J.; Singh, S.; Bhattacharya, S.; Noth, H. *Inorg. Chem.* **2011**, *50*, 10056−10069. (b) Zhang, Z.; Lim, W. P.; Wong, C. T.; Xu, H.; Yin, F.; Chin, W. S. *Nanomaterials* **2012**, *2*, 113−133.
(12) (a) Spicer, M. D.; Reglinski, J. *Eur. J. Inorg. Chem.* **2009**, 1553−1574. (b) Smith, J. M. *Comm. Inorg. Chem.* **2008**, *29*, 189−233. (c) Soares, L. F.; Silva, R. M. *Inorg. Synth.* **2002**, *33*, 199−202. (d) Rabinovich, D. *Struct. Bonding (Berlin, Ger.)* **2006**, *120*, 143−162.
(13) (a) Parkin, G. *New J. Chem.* **2007**, *31*, 1996−2014. (b) Parkin, G. *Chem. Rev.* **2004**, *104*, 699−767. (c) Parkin, G. *Chem. Commun.* **2000**, 1971−1985.
(14) (a) Vahrenkamp, H. *Acc. Chem. Res.* **1999**, *32*, 589−596. (b) Vahrenkamp, H. *Bioinorganic Chemistry—Transition Metals in Biology and their Coordination Chemistry;* Wiley-VCH: Weinheim, Germany, 1997; pp 540−551. (c) Vahrenkamp, H. *Dalton Trans.* **2007**, 4751−4759.
(15) Kreider-Mueller, A.; Rong, Y.; Owen, J. S.; Parkin, G. *Dalton Trans.* **2014**, *43*, 10852−10865.
(16) Rajesekharan-Nair, R.; Lutta, S. T.; Kennedy, A. R.; Reglinski, J.; Spicer, M. D. *Acta Crystallogr.* **2014**, *C70*, 421−427.
(17) (a) Green, M. L. H. *J. Organomet. Chem.* **1995**, *500*, 127−148. (b) Parkin, G. In Chapter 1.01. *Comprehensive Organometallic Chemistry III;* Crabtree, R. H., Mingos, D. M. P., Eds.; Elsevier: Oxford, U.K., 2007; Vol. *1*. (c) Green, J. C.; Green, M. L. H.; Parkin, G. *Chem. Commun.* **2012**, *48*, 11481−11503. (d) Green, M. L. H.; Parkin, G. *J. Chem. Educ.* **2014**, *91*, 807−816.
(18) (a) Melnick, J. G.; Zhu, G.; Buccella, D.; Parkin, G. *J. Inorg. Biochem.* **2006**, *100*, 1147−1154. (b) Melnick, J. G.; Docrat, A.; Parkin, G. *Chem. Commun.* **2004**, 2870−2871.
(19) For other {[Tm^{R}]Zn} complexes, see: (a) Bridgewater, B. M.; Parkin, G. *Inorg. Chem. Commun.* **2001**, *4*, 126−129. (b) Bridgewater, B. M.; Parkin, G. *J. Am. Chem. Soc.* **2000**, *122*, 7140−7141. (c) Bridgewater, B. M.; Fillebeen, T.; Friesner, R. A.; Parkin, G. *J. Chem. Soc., Dalton Trans.* **2000**, 4494−4496. (d) Morlok, M. M.; Janak, K. E.; Zhu, G.; Quarless, D. A.; Parkin, G. *J. Am. Chem. Soc.* **2005**, *127*, 14039−14050.
(20) Melnick, J. G.; Parkin, G. *Dalton Trans.* **2006**, 4207−4210.
(21) Rabinovich has also reported [TmBu^{t}]CdBr. See: White, J. L.; Tanski, J. M.; Rabinovich, D. *J. Chem. Soc., Dalton Trans.* **2002**, 2987−2991.
(22) (a) Melnick, J. G.; Parkin, G. *Science* **2007**, *317*, 225−227. (b) Melnick, J. G.; Yurkerwich, K.; Parkin, G. *Inorg. Chem.* **2009**, *48*, 6763−6772. (c) Melnick, J. G.; Yurkerwich, K.; Parkin, G. *J. Am. Chem. Soc.* **2010**, *132*, 647−655.
(23) (a) Manna, L.; Scher, E. C.; Alivisatos, A. P. *J. Am. Chem. Soc.* **2000**, *122*, 12700−12706. (b) Rosenthal, S. J.; McBride, J.; Pennycook, S. J.; Feldman, L. C. *Surf. Sci. Rep.* **2007**, *62*, 111−157. (c) Onodera, A.; Takesada, M. In *Advances in Ferroelectrics;* Barranco, A. P., Ed.; InTech: Rijeka, Croatia, 2013; Chapter 11.
(24) For other structurally characterized [Tm^{R}]CdX compounds, see: (a) Bakbak, S.; Incarvito, C. D.; Rheingold, A. L.; Rabinovich, D. *Inorg. Chem.* **2002**, *41*, 998−1001. (b) Cassidy, I.; Garner, M.; Kennedy, A. R.; Potts, G. B. S.; Reglinski, J.; Slavin, P. A.; Spicer, M. D. *Eur. J. Inorg. Chem.* **2002**, 1235−1239. (c) Bailey, P. J.; Dawson, A.; McCormack, C.; Moggach, S. A.; Oswald, I. D. H.; Parson, S.; Rankin, D. W. H.; Turner, A. *Inorg. Chem.* **2005**, *44*, 8884−8898. (d) Bakbak, S.; Bhatia, V. K.; Incarvito, C. D.; Rheingold, A. L.; Rabinovich, D. *Polyhedron* **2001**, *20*, 3343−3348. (e) Palmer, J. H.; Parkin, G. *Dalton Trans.* **2014**, *43*, 13874−13882.
(25) Tris(pyrazolyl)hydroborato cadmium acetate complexes have, nevertheless, been reported. See: (a) Darensbourg, D. J.; Niezgoda, S. A.; Holtcamp, M. W.; Draper, J. D.; Reibenspies, J. H. *Inorg. Chem.* **1997**, *36*, 2426−2432. (b) Darensbourg, D. J.; Holtcamp, M. W.; Khandelwal, B.; Klausmeyer, K.; Reibenspies, J. H. *J. Am. Chem. Soc.* **1995**, *117*, 538−539.
(26) Mihalcik, D. J.; White, J. L.; Tanski, J. M.; Zakharov, L. N.; Yap, G. P. A.; Incarvito, C. D.; Rheingold, A. L.; Rabinovich, D. *Dalton Trans.* **2004**, 1626−1634.
(27) These reactions can be performed by either (a) addition of RCO_2H to a mixture of [Tm$^{Bu^t}$]Na and Me_2Cd or by (b) treatment of RCO_2H with Me_2Cd, followed by addition of [Tm$^{Bu^t}$]Na.
(28) Kleywegt, G. J.; Wiesmeijer, W. G. R.; van Driel, G. J.; Driessen, W. L.; Reedijk, J.; Noordik, J. H. *J. Chem. Soc., Dalton Trans.* **1985**, 2177−2184.
(29) Addison, C. C.; Logan, N.; Wallwork, S. C.; Garner, C. D. *Quart. Rev. Chem. Soc.* **1971**, *25*, 289−322.
(30) Deacon, G. B.; Phillips, R. J. *Coord. Chem. Rev.* **1980**, *33*, 227−250.
(31) These values pertain to nonbridging carboxylate ligands.
(32) $\tau_5 = (\beta - \alpha)/60$, where $\beta - \alpha$ is the difference between the two largest angles. See: Addison, A. W.; Rao, T. N.; Reedijk, J.; Vanrijn, J.; Verschoor, G. C. *J. Chem. Soc., Dalton Trans.* **1984**, 1349−1356.
(33) Savant, V. V.; Gopalakr, J.; Patel, C. C. *Inorg. Chem.* **1970**, *9*, 748−751.
(34) Nyman, M. D.; Hampden-Smith, M. J.; Duesler, E. N. *Inorg. Chem.* **1997**, *36*, 2218−2224.
(35) Kireeva, I. K.; Mazo, G. Ya.; Schelokov, R. N. *Russ. J. Inorg. Chem.* **1979**, *24*, 220−225.
(36) Kato, S.; Niyomura, O. *Top. Curr. Chem.* **2005**, *251*, 13−85.
(37) Vallejo-Sanchez, D.; Beobide, G.; Castillo, O.; Lanchas, M. *Eur. J. Inorg. Chem.* **2013**, *2013*, 5592−5602.
(38) Furthermore, the Cd···O distance is also much greater than those in the carboxylate derivatives, [Tm$^{Bu^t}$]Cd(κ^2-O_2CR), described above (Table 1).
(39) Yang, L.; Powell, D. R.; Houser, R. P. *Dalton Trans.* **2007**, 955−64.
(40) Since [Tm$^{Bu^t}$]Cd[κ^1-SC(O)Ph] is the first reported structurally characterized cadmium thiobenzoate compound with an [S_4] coordination environment, there are no other similar compounds with which to compare this value.
(41) (a) Green, M. L. H. *J. Organomet. Chem.* **1995**, *500*, 127−148. (b) Parkin, G. Chapter 1. In *Comprehensive Organometallic Chemistry III;* Crabtree, R. H., Mingos, D. M. P., Eds.; Elsevier: Oxford, U.K., 2007; Vol. *1*. (c) Green, M. L. H.; Parkin, G. *J. Chem. Educ.* **2014**, *91*, 807−816.
(42) Cordero, B.; Gómez, V.; Platero-Prats, A. E.; Revés, M.; Echeverría, J.; Cremades, E.; Barragán, F.; Alvarez, S. *Dalton Trans.* **2008**, 2832−2838.
(43) Other coordination modes are known. See, for example, ref 10.
(44) Kunze, K.; Bihry, L.; Atanasova, P.; Hampden-Smith, M. J.; Duesler, E. N. *Chem. Vap. Deposition* **1996**, *2*, 105−108.
(45) *O*-unidentate coordination is, nevertheless, present in esters.

DOI: 10.1021/acs.inorgchem.5b00017
Inorg. Chem. 2015, 54, 3835−3850

(46) Vittal, J. J.; Sampanthar, J. T.; Lu, Z. *Inorg. Chim. Acta* **2003**, *343*, 224−230.
(47) Vittal, J. J.; Dean, P. A. W. *Acta Crystallogr.* **1997**, *C53*, 409−410.
(48) Parr, R. G.; Pearson, R. G. *J. Am. Chem. Soc.* **1983**, *105*, 7512−7516.
(49) For example, $H_2C{=}O$ (179.0 kcal mol-1), $H_2C{=}S$ (132 kcal mol^{-1}), $CH_3{-}OH$ (92.1 kcal mol-1), and $CH_3{-}SH$ (74.7 kcal mol-1). See: Wiberg, K. B.; Wang, Y. *ARKIVOC* **2011**, 45−56.
(50) Hadad, C. M.; Rablen, P. R.; Wiberg, K. B. *J. Org. Chem.* **1998**, *63*, 8668−8681.
(51) The thioxo form, RC(S)OH, is, however, predominant in polar solvents at low temperature, where hydrogen bonding interactions play an important role. See: Osamu, N.; Kato, S. *Top. Curr. Chem.* **2005**, *251*, 1−12.
(52) For example, the calculated G-2 bond dissociation energies for HC(O)O−H (111.2 kcal mol^{-1}) and HC(O)S−H (85.2 kcal mol^{-1}), respectively, differ by 26 kcal mol^{-1}. See ref 50.
(53) (a) Beeby, J.; Sternhell, S.; Hoffmann-Ostenhof, T.; Pretsch, E.; Simon, W. *Anal. Chem.* **1973**, *45*, 1571−1573. (b) Corio, P. L.; Dailey, B. P. *J. Am. Chem. Soc.* **1956**, *78*, 3043−3048.
(54) Bryant, R. G. *J. Chem. Educ.* **1983**, *60*, 933−935.
(55) For example, the rate constant at coalescence is predicted to be 910 s^{-1}. See ref 54.
(56) Specifically, the rate of exchange of a solution containing [$TmBu^t$] $Cd(O_2C$-*p*-Tol) (0.027 M) and *p*-$TolCO_2H$ (0.027 M) is 8 Ms^{-1}.
(57) (a) Chen, H.; Viel, S.; Ziarelli, F.; Peng, L. *Chem. Soc. Rev.* **2013**, *42*, 7971−7982. (b) Yu, J.-x.; Kodibagkar, V. D.; Cui, W.; Mason, R. P. *Curr. Med. Chem.* **2005**, *12*, 819−848.
(58) The assignments were made on the basis of C−F coupling constants (see, for example: Weigert, F. J.; Roberts, J. D. *J. Am. Chem. Soc.* **1971**, *93*, 2361−2369) and HSQC spectroscopy.
(59) At lower temperatures (183 K), a third species that is tentatively assigned as a hydrogen bonded adduct, [Tm^{Bu^t}]$Cd(\kappa^2$-$O_2CArF)\cdot HO_2CArF$, appears at −110.6 ppm.
(60) Budzelaar, P. H. M. *gNMR*, Version 5.0.1.0; Cherwell Scientific Publishing: Oxford Science Park, U.K., 2002.
(61) The derived rate values assume that interconversion between monomeric and dimeric forms of the carboxylic acid is rapid on the NMR time scale.
(62) Note that these representations for the possible transition state are only intended to be illustrative of composition. For example, it is also possible that the oxygen of R^*CO_2H that coordinates initially to cadmium is also the one that delivers the proton.
(63) Dissociation of [$ArFCO_2HO_2CArF$]$^-$ could also from [Tm^{Bu^t}] $Cd(\kappa^2$-$O_2CArF)\cdots HO_2CArF$ in a dissociative manner.
(64) Yoon, Y. H.; Lee, S. T.; Shieh, D. J.; Eyring, H.; Lin, S. H. *Chem. Phys. Lett.* **1976**, *38*, 24−27.
(65) (a) Davis, M. M.; Hetzer, H. B. *J. Res. Natl. Bur. Stand.* **1961**, *A 65*, 209−213. (b) Barela, R.; Buchowski, H.; Szatylowicz, H. *Fluid Phase Equilib.* **1994**, *92*, 303−312. (c) Long, B. W.; Wang, Y.; Yang, Z. R. *J. Chem. Thermodyn.* **2008**, *40*, 1565−1568. (d) Pham, H. H.; Taylor, C. D.; Henson, N. J. *J. Phys. Chem. B* **2013**, *117*, 868−876. (e) Barela, R.; Liwski, G.; Szatlowicz, H. *Fluid Phase Equilib.* **1995**, *105*, 119−127. (f) Muller, N.; Hughes, O. R. *J. Phys. Chem.* **1966**, *70*, 3975−3982. (g) Kimtys, L. L.; Balevicius, V. J. *Adv. Mol. Relax. Int. Proc.* **1979**, *15*, 151−161.
(66) The value of −16 e.u. corresponds to the average of a series of benzoic acid derivatives, which range from −13.7 to −17.9 e.u. See reference 65a.
(67) In view of the complex rate expression, activation parameters derived from the data in Table 7 are not reported.
(68) (a) Sharps, J. A.; Brown, G. E.; Stebbins, J. F. *Geochim. Cosmochim. Acta* **1993**, *57*, 721−731. (b) O'Reilly, D. E.; Schacher, G. E.; Schug, K. *J. Chem. Phys.* **1963**, *39*, 1756.
(69) (a) Cheesman, B. V.; Arnold, A. P.; Rabenstein, D. L. *J. Am. Chem. Soc.* **1988**, *110*, 6359−6364. (b) Rabenstein, D. L.; Reid, S. *Inorg. Chem.* **1984**, *23*, 1246−1250.
(70) Alouani, K.; Khaddar, M. R.; Chimie, D. De; Tunis, S. De; Rodehuser, L.; Rubini, P. R.; Sciences, F.; Cedex, V. *Polyhedron* **1985**, *4*, 643−647.
(71) (a) Reed, G. H.; Kula, R. J. *Inorg. Chem.* **1971**, *10*, 2050−2057. (b) Sudmeier, J. L.; Reilley, C. N. *Inorg. Chem.* **1966**, *5*, 1047−1055.
(72) Rabenstein, D. L.; Kula, R. J. *J. Am. Chem. Soc.* **1969**, *91*, 2492−2503.
(73) Eigen, M. *Pure Appl. Chem.* **1963**, *6*, 97−116.
(74) The proposal that the mechanism is dissociative was based on the suggestion that the concentration of [Na(kryptofix-221)][$Me^{13}CO_2$] was low and that steric interactions with the *t*-butyl substituents would inhibit an associative mechanism. However, other than demonstrating that the exchange is facile on the NMR time scale, the kinetics were neither quantified nor measured as a function of concentration because of solubility issues. See reference 25.
(75) (a) Lane, T. W.; Saito, M. A.; George, G. N.; Pickering, I. J.; Prince, R. C.; Morel, F. M. M. *Nature* **2005**, *435*, 42. (b) Lane, T. W.; Morel, F. M. M. *Proc. Natl. Acad. Sci. U. S. A.* **2000**, *97*, 4627−4631.
(76) Total concentration of $ArFCO_2H$ in monomeric and dimeric forms, that is, $[ArFCO_2H]_e + 2[(ArFCO_2H)_2]_e$.
(77) Galland, C.; Ghosh, Y.; Steinbrück, A.; Sykora, M.; Hollingsworth, J. A.; Klimov, V. I.; Htoon, H. *Nature* **2011**, *479*, 203−207.
(78) (a) McNally, J. P.; Leong, V. S.; Cooper, N. J. In *Experimental Organometallic Chemistry;* Wayda, A. L., Darensbourg, M. Y., Eds.; American Chemical Society: Washington, DC, 1987; Chapter 2, pp 6−23. (b) Burger, B. J.; Bercaw, J. E. In *Experimental Organometallic Chemistry;* Wayda, A. L., Darensbourg, M. Y., Eds.; American Chemical Society: Washington, DC, 1987; Chapter 4, pp 79−98. (c) Shriver, D. F.; Drezdon, M. A. *The Manipulation of Air-Sensitive Compounds,* 2nd ed.; Wiley-Interscience: New York, 1986.
(79) Gottlieb, H. E.; Kotlyar, V.; Nudelman, A. *J. Org. Chem.* **1997**, *62*, 7512−7515.
(80) Dungan, C. H.; van Wazer, J. R. *Compilation of Reported 19F NMR Chemical Shifts 1951 to mid 1967;* Wiley-Interscience: New York, 1970.
(81) (a) Sheldrick, G. M. *SHELXTL,* An Integrated System for Solving, Refining and Displaying Crystal Structures from Diffraction Data; University of Göttingen: Federal Republic of Germany, 1981. (b) Sheldrick, G. M. *Acta Crystallogr.* **2008**, *A64*, 112−122.
(82) Ammann, C.; Meier, P.; Merbach, A. E. *J. Magn. Reson.* **1982**, *46*, 319−321.

DOI: 10.1021/acs.inorgchem.5b00017
Inorg. Chem. 2015, 54, 3835−3850